Mechanisms of phosphate transport

Levi, Moshe ; Gratton, Enrico ; Forster, Ian C ; Hernando, Nati ; Wagner, Carsten A ; Biber, Juerg ; Sorribas, Victor ; Murer, Heini

Abstract: Over the past 25 years, successive cloning of SLC34A1, SLC34A2 and SLC34A3, which encode the sodium-dependent inorganic phosphate (P_i) cotransport proteins 2a-2c, has facilitated the identification of molecular mechanisms that underlie the regulation of renal and intestinal P_i transport. P_i and various hormones, including parathyroid hormone and phosphatonins, such as fibroblast growth factor 23, regulate the activity of these P_i transporters through transcriptional, translational and post-translational mechanisms involving interactions with PDZ domain-containing proteins, lipid microdomains and acute trafficking of the transporters via endocytosis and exocytosis. In humans and rodents, mutations in any of the three transporters lead to dysregulation of epithelial P_i transport with effects on serum P_i levels and can cause cardiovascular and musculoskeletal damage, illustrating the importance of these transporters in the maintenance of local and systemic P_i homeostasis. Functional and structural studies have provided insights into the mechanism by which these proteins transport P_i, whereas in vivo and ex vivo cell culture studies have identified several small molecules that can modify their transport function. These small molecules represent potential new drugs to help maintain P_i homeostasis in patients with chronic kidney disease - a condition that is associated with hyperphosphataemia and severe cardiovascular and skeletal consequences.

DOI: https://doi.org/10.1038/s41581-019-0159-y

Originally published at:
Levi, Moshe; Gratton, Enrico; Forster, Ian C; Hernando, Nati; Wagner, Carsten A; Biber, Juerg; Sorribas, Victor; Murer, Heini (2019). Mechanisms of phosphate transport. Nature Reviews. Nephrology, 15(8):482-500.
DOI: https://doi.org/10.1038/s41581-019-0159-y

Mechanismsofphosphatetransport

Moshe Levi [1], Enrico Gratton[2], Ian C. Forster [3], Nati Hernando[4], Carsten A. Wagner [4], Juerg Biber[4], Victor Sorribas[5] and Heini Murer[4]*

[1]Department of Biochemistry and Molecular & Cellular Biology, Georgetown University, Washington, DC, USA.

[2]Department of Biomedical Engineering, Laboratory for Fluorescence Dynamics, University of California– Irvine, Irvine, CA, USA.

[3]Florey Institute of Neuroscience and Mental Health, Parkville, Victoria, Australia.

[4]Institute of Physiology, University of Zurich, Zurich, Switzerland, and Swiss National Centres of Competence in Research, NCCR Kidney.CH, Zurich,

[5]Laboratory of Molecular Toxicology, Department of Toxicology, University of Zaragoza, Zaragoza, Spain.

**e-mail: Moshe.Levi@ georgetown.edu*

The authors contributed equally to all aspects of the article.

Abstract

Over the past 25 years, successive cloning of *SLC34A1*, *SLC34A2* and *SLC34A3*, which encode the sodium-dependent inorganic phosphate (P_i) cotransport proteins 2a–2c, has facilitated the identification of molecular mechanisms that underlie the regulation of renal and intestinal P_i transport. P_i and various hormones, including parathyroid hormone and phosphatonins, such as fibroblast growth factor 23, regulate the activity of these P_i transporters through transcriptional, translational and post-translational mechanisms involving interactions with PDZ domain-containing proteins, lipid microdomains and acute trafficking of the transporters via endocytosis and exocytosis. In humans and rodents, mutations in any of the three transporters lead to dysregulation of epithelial P_i transport with effects on serum P_i levels and can cause cardiovascular and musculoskeletal damage, illustrating the importance of these transporters in the maintenance of local and systemic P_i homeostasis. Functional and structural studies have provided insights into the mechanism by which these proteins transport P_i, whereas in vivo and ex vivo cell culture studies have identified several small molecules that can modify their transport function. These small molecules represent potential new drugs to help maintain P_i homeostasis in patients with chronic kidney disease — a condition that is associated with hyperphosphataemia and severe cardiovascular and skeletal consequences.

Key points

- In the past 25 years, the cloning of *SLC34A1*, *SLC34A2* and *SLC34A3*, which encode the Na^+-dependent inorganic phosphate (P_i) cotransporters NaPi-IIa, NaPi-IIb and NaPi-IIc, respectively, has enabled study of the molecular mechanisms that underlie the regulation of renal and intestinal P_i transport.
- Dietary factors, particularly dietary P_i, as well as hormones and phosphatonins, including parathyroid hormone (PTH) and fibroblast growth factor 23 (FGF23), regulate the expression and activity of the P_i transporters through transcriptional, translational and post-translational mechanisms that involve interactions with PDZ domain-containing proteins, lipid microdomains and acute trafficking via endocytosis or exocytosis.
- Mutations in any of the three transporters can cause dysregulation of epithelial P_i transport, can affect serum P_i levels and can cause damage of various target organs in both humans and rodents, highlighting the importance of these transporters in the maintenance of local and systemic P_i homeostasis.
- Functional studies together with structure–function studies have provided insights into the transport mechanisms of the NaPi-II cotransporter.
- The development of small molecules that modify the activity of P_i transporters holds promise for the maintenance of P_i homeostasis in patients with chronic kidney disease and other disorders associated with hyperphosphataemia and its severe cardiovascular and skeletal consequences.

Introduction

Since the identification of the major renal inorganic phosphate (P_i) transporter, encoded by *SLC34A1,* in 1993, advances in molecular and cell biology and biophysical and microscopy techniques have facilitated detailed study of the molecular mechanisms of renal and intestinal P_i transport. Impairment of renal and intestinal P_i transport results in hypophosphataemia, which leads to the dysfunction of several organ systems, including the musculoskeletal system. Conversely, dysregulation of renal and intestinal P_i transport, for example, as occurs in the setting of chronic kidney disease (CKD), results in hyperphosphataemia, which has major consequences for cardiovascular function and soft tissue calcification. Tight regulation of renal and intestinal P_i transport and P_i homeostasis is therefore crucial for normal organ function.

Before the identification of the P_i transporters, transport assays involving micropuncture of the intact renal proximal tubule and of isolated brush-border membrane vesicles (BBMVs) from renal and intestinal tissue identified the presence of a Na^+-dependent P_i flux across the luminal membranes of the respective epithelia[1,2,3]. These seminal investigations also provided new insights into the importance of the renal P_i reabsorption pathway in maintaining P_i homeostasis. Specifically, these studies demonstrated the dependence of renal P_i transport on parathyroid hormone (PTH), luminal pH and P_i itself[4,5]. However, many questions about the mechanisms of P_i transport remained unanswered; in particular, the molecular identity of the carrier proteins was unknown. In 1993, *SLC34A1*, which encodes the renal Na^+-dependent P_i cotransporter 2a (NaPi-IIa; also known as NPT2a), was successfully cloned from rat and human tissue using a *Xenopus laevis* oocyte expression system[6]. This success was followed in 1998 by the cloning of a second Na^+-dependent P_i cotransporter, NaPi-IIb (also known as NPT2b; encoded by *Slc34a2*) from mouse intestine[7]. The third member of the family, the renal NaPi-IIc (also known as NPT2c; encoded by *Slc34a3*), was cloned from mouse kidney tissue in 2002 (ref.[8]). These three isoforms have different tissue distributions, with NaPi-IIa and NaPi-IIc being expressed in kidney and NaPi-IIb being expressed in intestine and other tissues (Table 1). The critical role of the two renal isoforms in maintaining P_i homeostasis has been confirmed through gene knockout studies[9,10,11] and from studies of humans with naturally occurring mutations. In addition to NaPi-II transporters, the two members of the SLC20 family of Na–P_i cotransporters, namely, PIT1 (encoded by *SLC20A1*) and PIT2 (encoded by *SLC20A2*), are expressed (among other tissues) in renal and intestinal tissues, although their regulation and overall contribution to P_i homeostasis remains only partially understood[12].

Table 1 Properties of NaPi-II proteins

Properties	Isoform		
	NaPi-IIa (*SLC34A1*)	**NaPi-IIb (*SLC34A2*)**	**NaPi-IIc (*SLC34A3*)**
Tissue distribution	Kidney, bone	Gut, lung, liver, mammary gland, salivary gland, thyroid and testes	Kidney
Driving cations	Na^+ (Li^+)	Na^+(Li^+)	Na^+
Electrogenic (charge per cycle)	Yes (1)	Yes (1)	No (0)
Stoichiometry (Na:P_i)	3:1	3:1	2:1

NaPi, Na^+-dependent P_i cotransporter; P_i, inorganic phosphate.

In this Review, we describe the mechanisms by which dietary, hormonal and metabolic factors regulate the expression and function of NaPi-II transporters and how understanding of their structure–function relationships has provided insights into the mechanisms by which they transport P_i. We also discuss the consequences of dysregulated P_i transport and how the identification of small molecules that can modify P_i transport might aid in the development of new agents to maintain P_i homeostasis in patients with CKD.

Dietary factors and metabolic acidosis

P_i itself, including P_i from dietary sources, is a major regulator of NaPi-II transporter function. Moreover, dietary potassium (K) and changes in pH resulting from metabolic acidosis contribute to the regulation of P_i homeostasis.

Dietary P_i

Under normal physiological conditions and in the context of normal kidney function, maintenance of P_i homeostasis and serum P_i levels are primarily mediated through regulated reabsorption of P_i by the kidney and to a lesser extent through absorption of P_i in the intestine. Dietary P_i is a major regulator of renal P_i reabsorption. Dietary restriction of P_i results in a rapid adaptive increase in P_i reabsorption mediated by sequential upregulation of NaPi-IIa expression, followed by NaPi-IIc, and eventually PIT2 in the brush-border membrane (BBM) of the renal proximal tubule[8,13,14]. Conversely, ingestion of a high-P_i diet induces rapid downregulation of NaPi-IIa, followed by NaPi-IIc and PIT2 (ref.[14]). NaPi-IIa is not recycled, and after endosomal internalization it is degraded in lysosomes[15]. By contrast, NaPi-IIc accumulates subapically and is most likely partially recycled[16], although the renal adaptation of NaPi-IIc and PIT2 to dietary changes in P_i is not well understood. Trafficking of NaPi-IIa and NaPi-IIc to the apical BBM of proximal tubular epithelial cells in response to low dietary P_i involves microtubule-dependent translocation[16,17], as well as interactions of the transporters with the PDZ domain-containing proteins sodium–hydrogen antiporter 3 regulating factor 1 (NHERF1; also known as EBP50) and NHERF3 (also known as PDZK1)[18,19,20,21] (Fig. 1), as discussed later.

The adaptation of renal P_i reabsorption to acute variations in dietary P_i levels does not involve alterations in RNA levels of the transporters. However, persistent changes in P_i concentration as a result of chronic alterations in dietary P_i intake alter the transcription and translation of NaPi transporters, leading to increased or decreased RNA and protein levels[22]. The adaptive changes of the kidney to acute and chronic dietary P_i are accompanied by modifications in the concentration of several hormones and other factors such as PTH, fibroblast growth factor 23 (FGF23), 1,25-dihydroxy-vitamin D_3 ($1,25(OH)_2D_3$), insulin and dopamine (reviewed elsewhere[23,24]). However, only PTH seems to be necessary for the early adaptation of renal NaPi transport to high dietary P_i (ref.[25]) (discussed later).

Dietary potassium

K^+ deficiency and resultant hypokalaemia occur as a consequence of decreased dietary intake, decreased intestinal K^+ absorption and increased urinary K^+ secretion resulting from diuretic use or tubular transport defects. Deficiency of K induces an increase in urinary P_i excretion that is mediated, at least in part, via decreased Na–P_i cotransport activity in the BBM of the renal proximal tubule[26]. This decrease in Na–P_i cotransport activity occurs despite increased BBM expression of NaPi-IIa and PIT1 owing to a decrease in the lateral diffusion and increased clustering of these transporters in the BBM, hindering their activity[27]. By contrast, dietary K^+ deficiency decreases BBM expression of NaPi-IIc and PIT2 (ref.[28]), suggesting that the mechanisms by which dietary K^+ regulates Na–P_i transport are complex.

Metabolic acidosis

Metabolic acidosis increases urinary excretion of P_i, which aids the removal of acid from the blood[29,30]. However, studies into the mechanisms underlying the phosphaturia have yielded conflicting findings. In rats, chronic metabolic acidosis (for ≥ 12 h) achieved by administration of NH_4Cl in both food and drinking water led to progressively decreased BBM Na–P_i cotransport activity as a result of impaired transcription and translation of NaPi-IIa[29]. These effects of metabolic acidosis on NaPi transporter expression are blunted by a low-P_i diet, which counteracts the effects of acidosis on NaPi-IIa expression[31]. Rats with acute metabolic acidosis (for ≤ 6 h) also exhibit a decrease in BBM Na–P_i cotransport activity; however, this decrease is independent of changes in *Slc34a1* mRNA expression[29]. Rather, the decrease in NaPi-IIa protein expression resulting from acute metabolic acidosis is probably mediated by changes in NaPi-IIa trafficking through enhanced internalization from and/or impaired delivery of NaPi-IIa to the apical BBM[29,31]. Another study showed that unlike wild-type mice, NaPi-IIa-null mice do not exhibit a transient increase in urinary P_i excretion in response to 2 days of acid loading[30]. However, in contrast to the above-described studies[29,31], this study found that acidosis increased the expression of NaPi-IIa in the BBM of wild-type mice and the expression of NaPi-IIc in both wild-type and NaPi-IIa-null animals[30]. The phosphaturia observed during acidosis might therefore not be a consequence of reduced transporter expression but rather result from a direct inhibitory effect of acidosis on transport function[30].

Regulation of NaPi-II by hormones

The capacity of the kidney to reabsorb P_i is under tight hormonal control. This control is mostly mediated via hormonally induced regulation of the abundance of NaPi-II cotransporters in the proximal tubule BBM.

PTH

PTH is an important regulator of Na–P_i cotransport. It markedly increases urinary P_i excretion and decreases renal P_i reabsorption by altering the abundance of NaPi-IIa, NaPi-IIc and PIT2 in the BBM. Administration of PTH to mice and rats induces rapid (within minutes) removal of NaPi-IIa protein from the BBM without any corresponding change in mRNA levels[17,32,33]. Likewise, PIT2 is removed from the BBM of mice within

60 min of PTH treatment[34]. However, PTH-induced removal of NaPi-IIc from the BBM takes hours[35], as discussed below.

The removal of NaPi-IIa from the BBM in response to PTH requires phosphorylation of the PDZ domain-containing protein NHERF1 (ref.[36]). This phosphorylation destabilizes the association of NHERF1 with NaPi-IIa, allowing removal of the cotransporter from the BBM[19]. Notably, several point mutations in *NHERF1* (also known as *SLC9A3R1*) have been identified in humans, some of whom have nephrolithiasis or bone mineralization defects[37]. Transfection of mutant *NHERF1* cDNA into a kidney tubule cell line increased the responsiveness of NaPi-IIa to PTH, resulting in a significant decrease in phosphate uptake and suggesting that mutations of *NHERF1* might contribute to the pathogenesis of renal loss of P_i (ref.[37]).

In addition to regulating the trafficking and stabilization of NaPi-IIa in the apical BBM, NHERF1 also mediates PTH-receptor-induced activation of phospholipase C (PLC), which is important for PTH-mediated internalization of NaPi-IIa[38,39,40]. Several signalling cascades are involved in the PTH-induced removal of NaPi-IIa from the BBM. PTH signals through PTH1 receptors located at the apical and basolateral membranes of the renal proximal tubule. Activation of basolateral PTH1 receptors increases cAMP levels and stimulates protein kinase A (PKA)-dependent pathways, whereas activation of apical PTH1 receptors couples to PLC and therefore results in hydrolysis of phosphatidylinositol 4,5-bisphosphate (PtdIns(4,5)P_2) and activation of protein kinase C (PKC)[34,41]. NHERF1, which is specifically expressed in the apical membrane, links the PTH1 receptors with PLC and is responsible for the different intracellular signalling elicited by apical and basolateral receptors[39]. The response of NaPi-IIc to PTH also involves PKA and PKC because downregulation of the cotransporter is observed in mice following administration of PTH fragments that activate only PKC or PKA and PKC[34,35]. In addition to PKA and PKC, the mitogen-activated protein kinases extracellular-signal regulated kinase 1 (ERK1) and ERK2 are thought to contribute to PTH-induced regulation of Na–P_i cotransport[42,43].

After its removal from the BBM in response to PTH, NaPi-IIa is transported via clathrin-coated pits to early and late endosomes and then to lysosomes for degradation[17,44,45]. By contrast, although treatment with PTH induces internalization of NaPi-IIc[35] and PIT2 (ref.[34]), the fate of these transporters remains unknown.

As mentioned above, PTH induces a rapid decrease in the expression of NaPi-IIa protein in the BBM through endocytosis. Concomitantly, NaPi-IIa accumulates in endosomes, whereas microtubules form dense bundles in an apical-to-basal orientation[46]. This bundling of microtubules is thought to be a general feature of rapid endocytosis, and it is consistent with microtubular-dependent trafficking of internalized cotransporters along the endocytic pathway. After 60 min of PTH action, the tubule cells are vastly depleted of NaPi-IIa owing to lysosomal degradation of internalized transporters, at which point their microtubular cytoskeleton returns to normal[46]. Prevention of the microtubule rearrangement by administration of the microtubule-stabilizing agent paclitaxel induced NaPi-IIa to accumulate in the subapical portion of the cell, delaying its depletion[46]. The accumulation of NaPi-IIa in the subapical portion of the cell was associated with expansion of the dense apical tubules of the subapical endocytic apparatus (SEA), suggesting that PTH-induced downregulation of NaPi-IIa

occurs through an endocytic process that involves internalization of the transporter into the SEA and delivery of the transporter to lysosomes for degradation[46].

Use of total internal reflection fluorescence (TIRF) microscopy has shown that a dynamic actin cytoskeleton is required for the removal of NaPi-IIa from the BBM in response to PTH. In addition, these imaging studies have shown that myosin VI — a myosin motor that is co-regulated with NaPi-IIa — is necessary for PTH-induced removal of NaPi-IIa from BBM microvilli[47].

A number of imaging techniques, including TIRF, modulation tracking (or nanoscale precise imaging by rapid beam oscillation (nSPIRO)), raster image correlation spectroscopy (RICS) and number and brightness (N&B) analysis, have been used to study the differential modulation of NaPi-IIa and NaPi-IIc by PTH. These studies have demonstrated that expression of both NaPi-IIa and NaPi-IIc in the apical membrane of renal proximal tubule cells is decreased in response to PTH, but as mentioned earlier, the removal of NaPi-IIc from the apical BBM is much slower than for NaPi-IIa[48]. Analysis of the diffusion coefficients of the two transporters suggests that NaPi-IIc remains tethered within the apical membrane for longer than NaPi-IIa following PTH treatment, accounting, at least in part, for the difference between the two transporters in their response to PTH[48] (Fig. 1).

1,25-Dihydroxy-vitamin D_3

The active form of vitamin D, $1,25(OH)_2D_3$, has also been shown to increase proximal tubular P_i reabsorption[49]. Compared with levels in wild-type mice, concentrations of $1,25(OH)_2D_3$ are elevated in NaPi-IIa-deficient mice, presumably to compensate for urinary P_i waste[50]. Whether $1,25(OH)_2D_3$ has direct effects on NaPi transporters is, however, controversial as vitamin D status is closely associated with alterations in plasma levels of Ca^{2+}, PTH, FGF23 and Klotho — factors that all affect P_i transport. $1,25(OH)_2D_3$ also increases intestinal P_i absorption. Interestingly, both intestinal and renal adaptations to a low-P_i diet are conserved in vitamin D_3 receptor (VDR)-knockout mice[51]; however, these mice exhibit hypophosphataemia and hyperphosphaturia[51], suggesting that renal tubular P_i reabsorption is impaired. Compared with age-matched wild-type mice, VDR-knockout mice demonstrate decreased renal Na–P_i cotransport activity and considerably lower NaPi-IIa, NaPi-IIc and PIT2 protein levels following weaning[52]. However, intervention with a rescue diet containing a higher proportion of P_i and Ca^{2+} content to normalize PTH levels also normalized expression of the three transporters, indicating that lack of VDR activity per se does not impair renal P_i reabsorption.

Glucocorticoids

Glucocorticoids, including cortisone and dexamethasone, inhibit proximal tubule Na–P_i transport in mice, rats and humans[53,54]. Conversely, adrenalectomy increases P_i reabsorption[55]. In rats, chronic dexamethasone treatment decreases Na–P_i transport by decreasing NaPi-IIa mRNA and protein expression in the BBM[56]. In line with the renal effects, glucocorticoids also inhibit intestinal P_i absorption, as well as the RNA and protein abundance of NaPi-IIb[57].

Oestrogen

Oestrogen treatment has long been known to cause hypophosphataemia in humans[58]. Prolonged treatment of ovariectomized rats with oestrogen also decreases renal P_i reabsorption and results in hypophosphataemia. This decrease in proximal tubule P_i uptake is primarily the result of decreased NaPi-IIa mRNA and protein levels because NaPi-IIc expression is not affected[59]. In contrast to their effects in the kidney, oestrogens increase the intestinal absorption of P_i by increasing the RNA and protein expression of NaPi-IIb; however, this effect is not sufficient to counteract the hypophosphataemia resulting from the diminished renal expression of NaPi-IIa[60]. The effects of oestrogen on NaPi transporter expression are mediated by ERα and ERβ[61]. The phosphaturic effect of oestrogen might also be mediated through an increase in FGF23 synthesis, which results in decreased serum $1,25(OH)_2D_3$ and P_i levels[62]; however, this indirect mechanism of action does not seem to operate in the intestine because administration of oestrogens increases P_i uptake in the Caco-2 intestinal cells in vitro[60].

Thyroid hormone

Excess levels of thyroid hormone are associated with hyperphosphataemia[63]. Chronic treatment of thyroparathyroidectomized (TPTX) rats with thyroid hormone increases renal Na–P_i cotransport by increasing *Slc34a1* mRNA transcription and levels of NaPi-IIa protein in the BBM[63]. The NaPi-IIa gene, *SLC34A1*, contains a thyroid hormone response element, and administration of thyroid hormone to opossum kidney (OK) tubule cells increases NaPi-IIa expression, suggesting that the effects of thyroid hormone on this NaPi transporter are direct and independent of other hormones[64]. In addition to maintaining a basal level of phosphataemia through regulation of NaPi-IIa transcription, thyroid hormone seems to participate in the upregulation of P_i transport and NaPi-IIa expression at weaning because levels of the hormone and transporter are simultaneously increased in the transition between suckling and weaning in rats[65].

Regulation of NaPi by phosphatonins

The term phosphatonins describes several factors that, in addition to PTH and $1,25(OH)_2D_3$, regulate P_i homeostasis. This family includes FGF23, polypeptide *N*-acetylgalactosaminyltransferase 3 (GALNT3), phosphate-regulating neutral endopeptidase (PHEX), matrix extracellular phosphoglycoprotein (MEPE), dentin matrix acidic phosphoprotein 1 (DMP1), FGF7 and secreted frizzled-related protein 4 (sFRP4).

FGF23

FGF23 is a hormone that is synthesized by osteocytes and osteoblasts. The mature (active) form of FGF23 (also termed ‘intact’ FGF23) is generated following removal of the 24-residue signal peptide at the amino terminal. Intact FGF23 can also undergo cleavage at a furin-like cleavage site ($R_{176}XXR_{179}$) to produce inactive amino-terminal and carboxy-terminal fragments. As discussed below, the identity of the endopeptidase responsible for cleaving FGF23 remains a matter of debate. A glycosylation site at T178 overlaps with the furin-like cleavage site, and *O*-

glycosylation of intact FGF23 blunts this cleavage, promoting the secretion of intact FGF23 (reviewed elsewhere[66]). Carboxy-terminal fragments can compete with the intact hormone for binding to FGF receptor (FGFR)–α-Klotho complexes and thereby antagonize intact FGF23 signalling. FGF23 synthesis is stimulated by high dietary or plasma P_i levels[67] and by PTH[68], $1,25(OH)_2D_3$ (ref.[69]) and Ca^{2+} (ref.[70]). A number of other regulators have been identified in the past few years, including iron deficiency[71], erythropoietin[72], insulin[73], AMP kinase[74] and inflammatory cytokines[75].

FGF23 signalling requires the binding of the hormone to FGFR and α-Klotho[76], leading to activation of FGFR substrate 2α (FRS2α), ERK1 and/or ERK2 and serum/glucocorticoid regulated kinase 1 (SGK1). FGF23 reduces reabsorption of P_i in the renal proximal tubule and reduces levels of $1,25(OH)_2D_3$ by inhibiting renal $1,25(OH)_2D_3$ synthesis by CYP27B1 and enhancing $1,25(OH)_2D_3$ catabolism by CYP24A1 (ref.[77]). Because $1,25(OH)_2D_3$ also stimulates intestinal absorption of P_i, its reduction decreases active P_i absorption. FGF23 also downregulates the abundance of NaPi-IIa, NaPi-IIc and PIT2 in the proximal tubule. The combined effect of blunted intestinal and renal (re)absorption is a reduction in plasma levels of P_i. Similar to PTH, FGF23 destabilizes the anchoring of NaPi-IIa to the apical membrane by promoting the phosphorylation of NHERF1 (ref.[78]). Whether the different Na–P_i cotransporters exhibit different kinetics in response to FGF23 as they do for PTH is currently unknown.

Whereas PTH stimulates the production of FGF23, FGF23 negatively regulates the parathyroid gland, acting to inhibit the synthesis and/or release of PTH[79]. Studies in humans[80] and rodents[25] indicate that P_i loading induces an initial raise in plasma PTH levels, which precedes the increase in FGF23. In the absence of parathyroid glands, however, secretion of FGF23 may be accelerated[25]. Moreover, increased FGF23 precedes the development of hyperparathyroidism in patients with CKD and acute kidney injury, suggesting that under some circumstances changes in FGF23 may precede the elevation in PTH[81].

Mutations within the $R_{176}XXR_{179}$ cleavage motif that enhance the half-life of intact FGF23 result in excessive urinary P_i loss and cause autosomal dominant hypophosphataemic rickets (ADHR; OMIM 193100)[82]. Secretion of high levels of FGF23 by mesenchymal tumours is one cause of tumour-induced osteomalacia (also known as oncogenic hypophosphataemic osteomalacia (OHO; OMIM 605912)), which presents with hypophosphataemia secondary to renal P_i wasting and inappropriately normal or even low $1,25(OH)_2D_3$ levels[83]. Conversely, loss-of-function mutations in FGF23 cause familial tumoural calcinosis (FTC; OMIM 211900), which is characterized by reduced urinary excretion of P_i, hyperphosphataemia, normal or elevated $1,25(OH)_2D_3$ levels and ectopic calcification[84]. FTC can also be caused by mutations in α-Klotho[85]. FGF23-deficient and α-Klotho-hypomorphic mice exhibit hyperphosphataemia, reduced urinary P_i excretion, increased expression of NaPi-IIa and NaPi-IIc at the BBM and high $1,25(OH)_2D_3$ levels[86].

The effect of FGF23 on renal Na–P_i cotransporter expression largely depends on the presence of FGFR1 (ref.[87]), although a contribution of FGFR4 has also been reported[88]. FGFR1 probably also contributes to the FGF23-induced downregulation of PTH because this receptor (and α-Klotho) is downregulated in hyperplastic parathyroid glands from patients with uraemia[89]. In humans, gain-of-function mutations of FGFR1

cause osteoglophonic dysplasia (OMIM 166250), which is associated with hypophosphataemia as a result of massive urinary P_i loss[90].

A cleaved form of α-Klotho called soluble α-Klotho, which lacks co-receptor activity and is present in plasma and urine, promotes phosphaturia and downregulates NaPi-IIa even in the absence of FGF23 through a proteolytic mechanism that is dependent on its glucuronidase activity[91]. However, the crystal structure of a ternary complex consisting of human FGF23, the ligand-binding domain of FGFR1c and cleaved α-Klotho suggests that the structure of α-Klotho within this complex cannot support glycosidase activity[92]. Thus, the effect of α-Klotho on FGF23 signalling seems to be independent of its enzymatic activity. Of note, whereas inactivating mutations in α-Klotho can cause FTC[85], a translocation mutation that results in high levels of α-Klotho causes hypophosphataemic rickets and hyperparathyroidism[93].

GALNT3

GALNT3 is the glycosyltransferase that is responsible for *O*-glycosylation of FGF23 at T178, preventing its proteolytic processing and therefore allowing the secretion of intact FGF23 (ref.[94]). Mutations in GALNT3 are associated with FTC[95]. GALNT3-deficient mice have reduced circulating levels of intact FGF23 (ref.[96]); they are also hyperphosphataemic, have inappropriately normal levels of $1,25(OH)_2D_3$, reduced PTH and moderately upregulated *Slc34a1* mRNA expression. Homozygous GALNT3-deficient males are growth retarded and have increased bone mineral density. These phenotypes are partially normalized upon breeding with transgenic animals expressing a proteolysis-resistant form of human FGF23 ($Arg_{176}Gln$) found in some patients with ADHR[97], further suggesting that the GALNT3 transferase is required for proper secretion of intact FGF23.

GALNT3 mRNA expression is stimulated by extracellular P_i and by $1,25(OH)_2D_3$ in vitro[98]. Despite its stimulatory effect on FGF23 production, PTH inhibits expression of *Galnt3* mRNA in mice[99]. Reduced GALNT3 results in higher levels of FGF7 (see below) and matrix metalloproteinases MMP8 and MMP9, which are both involved in ectopic calcification[100].

PHEX

PHEX is a metalloendopeptidase that is mutated in patients with X-linked hypophosphataemic rickets (XLH; OMIM 307800)[101], a condition characterized by high FGF23 levels, hyperphosphaturia, hypophosphataemia, rickets, short stature and limb deformities. The *PHEX* gene is located on the X chromosome and regulates the expression but not the degradation of FGF23. As discussed below, PHEX recognizes particular motifs (acidic serine aspartate-rich MEPE-associated motifs (ASARMs)) found in short integrin-binding ligand-interacting glycoproteins (SIBLING) proteins (reviewed elsewhere[102]). The expression of PHEX is downregulated by $1,25(OH)_2D_3$ in osteoblastic cell lines, whereas in osteocyte-like cells it is upregulated by extracellular P_i and $1,25(OH)_2D_3$. Several mouse models carrying *Phex* mutations recapitulate the phenotype of XLH. In Hyp mice, for example (which have a mutation in *Phex*), urinary P_i loss correlates with elevated FGF23 levels and reduced expression of NaPi-IIa and NaPi-IIc at the renal proximal BBM[103]. Although PHEX was initially thought to be the protease responsible for FGF23 cleavage at the furin-like cleavage

site, and thus inactivation of FGF23, current evidence suggests that the pro-protein convertase complex 7B2–PC2 mediates FGF23 degradation[104], although this proposal needs further confirmation. Expression of the PC2 co-activator 7B2 and the active PC2 convertase are reduced in bones from Hyp mice, suggesting that the absence of PHEX impairs the cleavage of proPC2 and reduces 7B2–PC2 activity, thus providing a potential link between PHEX and FGF23 processing[104]. This hypothesis is supported by the finding that normalization of 7B2 levels in Hyp mice improves bone mineralization and increases plasma P_i levels and expression of NaPi-IIa owing to normalization (that is, a reduction) of FGF23 levels[104].

MEPE

MEPE is normally produced by osteoblast and osteocytes and is overexpressed in patients with tumour-induced osteomalacia[105]. MEPE belongs to the SIBLING family of proteins, the members of which are all the products of genes located on the same chromosome (5q in mouse and 4q in humans). All of these proteins are involved in regulating P_i, bone mineralization and extravascular mineralization and contain RGD (Arg, Gly and Asp) and ASARM domains. Upon proteolytic cleavage by cathepsin-like proteases, free ASARM peptides are released into the circulation. ASARM peptides increase plasma FGF23 levels and reduce expression of NaPi-IIa, thereby reducing plasma P_i levels and promoting fractional excretion of P_i, consequently inhibiting bone mineralization (reviewed elsewhere[102]). The interaction of PHEX with the ASARM domain of MEPE might prevent MEPE proteolysis by cathepsin-like proteases, preventing the release of ASARM peptides. PHEX can also bind to and hydrolyse free ASARM peptides, thus neutralizing their activity. Serum levels of MEPE-derived ASARM peptides are increased in Hyp mice and might contribute to their phosphaturia and impaired mineralization[106]. Administration of MEPE to mice and rats induces phosphaturia and reduces the expression of NaPi-IIa without changing the abundance of NaPi-IIc[107,108]. The expression of MEPE in osteocyte-like cells is upregulated by extracellular P_i (ref.[98]), and high dietary P_i increases MEPE expression in nephrectomized rats[109]. In addition, $1,25(OH)_2D_3$ stimulates MEPE expression in osteocyte-like cells[98] but reduces it in osteoblasts[110].

DMP1

DMP1 is another SIBLING protein that is produced by osteoblast and osteocytes and is overexpressed in patients with OHO[111]. In addition, DMP1 is mutated in patients with autosomal recessive hypophosphataemic rickets (ARHR1; OMIM 241520)[112,113]. Patients with ARHR1 present with hypophosphataemia and hyperphosphaturia, inappropriately normal levels of $1,25(OH)_2D_3$, high levels of FGF23 and severe rickets or osteomalacia, features that are reproduced in DPM1-deficient mice[113]. High circulating levels of DMP1-derived ASARM peptides are detected in Hyp mice. Deletion of *Dpm1* in Hyp mice does not cause additive changes in FGF23 or plasma P_i levels as compared with single mutants, indicating that PHEX and DMP1 use a common pathway to regulate FGF23 expression[114]. The expression of DMP1 in cultured bone cells is repressed by PTH and $1,25(OH)_2D_3$ (ref.[115]).

sFRP4

sFRP4 is a secreted member of the frizzled family; it is overexpressed (and secreted at high levels) in some tumours and associates with tumour-induced osteomalacia and OHO[116]. The physiological effects of sFRP4 probably depend on the extent of competition with membrane-bound frizzled receptors for binding to Wnt proteins[117]. Infusion of sFRP4 induces phosphaturia in intact and parathyroidectomized rats, paralleled by endocytic retrieval of NaPi-IIa[116]. Transgenic mice overexpressing sFRP4 postnatally have normal serum and urinary P_i levels, high $1,25(OH)_2D_3$ levels and high expression of *Slc34a1* mRNA, as well as impaired bone mineralization, and ablation of sFRP4 in mice does not alter serum or urinary P_i levels[118]. Thus, sFRP4 may control bone mineralization but not P_i homeostasis.

FGF7

FGF7 is a member of the FGF family of proteins, the members of which are secreted by the mesenchyme and contribute to the regulated development of organs, glands and limbs[119]. One study found that levels of FGF7 were upregulated in cultures established from OHO-associated tumours and that FGF7 had a potent inhibitory effect on P_i transport in renal proximal cells in vitro[120].

NaPi–PDZ protein interactions

The export and import of NaPi-II cotransporters to and from the cell membrane is achieved through interactions with proteins, including several PDZ domain-containing proteins[121]. PDZ domains are ~90 amino acids long, and their most common function is the formation of a molecular scaffold that anchors membrane proteins to the cytoskeleton[122]. Using the carboxyl terminus of NaPi-IIa as bait in a yeast two-hybrid screen, the first PDZ proteins to be identified as NaPi-IIa partners were NHERF1 (ref.[123]) and NHERF3 (refs[124,125,126,127]). Other PDZ proteins that bind the carboxyl terminus of NaPi-IIa are NHERF2 (also known as E3KARP)[128], NHERF4 (also known as PDZK2), SHANK2 (ref.[129]) and CFTR-associated ligand (CAL; also known as PIST)[130] (Fig. 2).

The carboxyl terminus of NaPi-IIa contains a class I PDZ-binding site, and the three amino acids at the end of this region (Thr-Arg-Leu) are necessary for interactions with PDZ domain-containing proteins. The three amino acids at the carboxyl terminus of NaPi-IIc are Gln-Gln-Leu in humans and in mouse and rat orthologues; this sequence enables NaPi-IIc to interact with NHERF1 and NHERF3 but does not enable interaction with NHERF2, NHERF4, CAL and SHANK[131] (Fig. 2). The interaction of NaPi-IIc with NHERF1 is maintained in the absence of the Gln-Gln-Leu motif.

NHERF1

NHERF1 contains two PDZ domains and an ezrin-radixin-moesin-binding domain (ERM-BD) at the carboxyl terminus that binds to the actin cytoskeleton (Fig. 2). NaPi-IIa binds only to the first PDZ domain of NHERF1, and this interaction is necessary for correct insertion of the cotransporter at the apical membrane[132]. In fact, targeted disruption of NHERF1 in mice reduces the expression of NaPi-IIa at the BBM; causes

hypophosphataemia and hyperphosphaturia; and attenuates the response of the remaining cotransporter to PTH, FGF23 and dietary P_i (ref.[133]). In agreement with this response, PTH and FGF23 phosphorylate NHERF1, causing it to dissociate from NaPi-IIa, leading to NaPi-IIa internalization; these actions require the formation of a ternary complex involving the PKA-anchoring protein ezrin, NHERF1 and NaPi-IIa[134]. As indicated earlier, NHERF1 also controls the intracellular signalling activated by PTH. In the absence of NHERF1, PTH1 receptors in the basolateral membrane of renal proximal tubules mostly stimulate PKA-dependent pathways. By contrast, the presence of NHERF1 in the apical BBM mediates the physical connection of the receptors with PLC, resulting in preferential activation of PLC and PKC[39]. Activation of PKA and PKC (as well as ERK) leads to phosphorylation of NHERF1, thus destabilizing its association with NaPi-IIa and enabling the endocytosis of the cotransporter[19,42]. In the intestine, NaPi-IIb interacts with NHERF1 but not with NHERF3 (ref.[135]). NHERF1 is involved in the adaptation of NaPi-IIb to changes in dietary P_i concentration.

NHERF3

The interaction of NaPi-IIa with NHERF3 has different consequences than the interaction with NHERF1. NHERF3 has four PDZ domains (the third of which interacts with NaPi-IIa) but lacks an ERM-BD (Fig. 2). Nevertheless, NHERF3 also binds to the actin cytoskeleton by interacting with NHERF1 or NHERF2 (ref.[136]). PTH does not phosphorylate NHERF3, suggesting that disassembly of the NaPi-IIa–NHERF3 complex occurs through different mechanisms than dissociation of NaPi-IIa from NHERF1 (ref.[137]). NHERF3-deficient mice have normal expression of NaPi-IIa at the proximal tubule BBM and exhibit normal regulation of NaPi-IIa by PTH and dietary P_i (refs[21,138]). However, NHERF3 seems to stabilize NaPi-IIc in the BBM. Use of fluorescence lifetime imaging microscopy and Förster resonance energy transfer (FLIM-FRET) demonstrated that the interaction of NHERF1 with NaPi-IIa is much stronger than that of NHERF1 with NaPi-IIc, whereas NHERF3 interacts with both with the same efficiency[138].

SHANK2E

SHANK2E is a single PDZ-containing protein that is expressed at the BBM of proximal tubules where it interacts with and contributes to the apical retention of NaPi-IIa[139,140] (Fig. 2). Unlike the above-mentioned PDZ partners, SHANK2 redistributes intracellularly with NaPi-IIa upon exposure to high P_i levels.

CAL

Similar to SHANK2E, CAL is an additional single PDZ-containing protein that interacts with NaPi-IIa[130,141] (Fig. 2). CAL is mainly located in the *trans*-Golgi network, where it partially colocalizes and interacts with NaPi-IIa. Although it has been proposed to retain NaPi-IIa in the *trans*-Golgi network, the exact role of CAL in the regulation of subcellular NaPi-IIa is unclear.

BBM lipid composition and lipid rafts

The first evidence for a role for lipids in modulating Na–P_i cotransport activity came from studies in ageing rats, which exhibit impaired renal tubular P_i transport[142]. This impairment is thought to result from two complementary mechanisms. The first is a decrease in the mRNA levels and protein abundance of NaPi-IIa at the tubule epithelial BBM[63,143]. The second mechanism involves post-transcriptional and post-translational regulation of NaPi-IIa through alterations in the lipid composition of the BBM. These lipid alterations, which particularly involve cholesterol, regulate NaPi-IIa abundance and activity through multiple mechanisms that affect processes such as transporter trafficking, diffusion and clustering[144].

Levels of cholesterol and sphingomyelin are increased in the tubule epithelial BBM of aged rats, and this increase is associated with decreased BBM fluidity as determined by measuring the fluorescence anisotropy of diphenylhexatriene. The BBM lipid composition and alterations in BBM fluidity also contribute to the impaired renal adaptation of NaPi-IIa transporters to a low-P_i diet in aged rats. Adult rats adapt to a low-P_i diet by decreasing BBM cholesterol levels and increasing BBM fluidity. In aged rats, however, the renal adaptation to a low-P_i diet is incomplete as the ability to lower BBM cholesterol and increase BBM fluidity is impaired[142]. Thus, the increase in BBM cholesterol content observed in aged rats and the associated decrease in BBM fluidity are important contributors to the impaired renal tubular P_i transport and adaptation to a low-P_i diet[142].

In vitro studies show that enrichment of renal BBM with cholesterol directly modulates Na–P_i cotransport, inducing a dose-dependent decrease in Na–P_i cotransport activity, which is paralleled by decreased BBM fluidity[145]. Increasing ambient temperature, which increases BBM fluidity independent of changes in cholesterol content, increases Na–P_i cotransport activity, indicating a direct link between BBM fluidity and Na–P_i cotransporter function; however, assessment of Na–P_i cotransport activity as a function of BBM fluidity shows that at equivalent BBM fluidities, BBM cholesterol enrichment results in a dose-dependent decrease in Na–P_i cotransport activity. Moreover, cholesterol enrichment of BBM isolated from rats fed a low-P_i diet completely reverses the adaptive increases in Na–P_i cotransport activity and BBM fluidity[145].

In line with the above findings, alterations in cellular cholesterol content also directly modulate Na–P_i cotransport activity and apical membrane NaPi-IIa protein expression in OK kidney tubule cells[144]. Acute depletion of cholesterol depletion achieved with β-methyl cyclodextrin results in increased Na–P_i cotransport activity accompanied by a moderate increase in apical membrane NaPi-IIa protein abundance and no alteration in the total cellular abundance of NaPi-IIa protein. Conversely, acute cholesterol enrichment decreases Na–P_i cotransport activity accompanied by a moderate decrease in apical membrane NaPi-IIa protein abundance and no change in the total cellular abundance of NaPi-IIa protein. By contrast, chronic cholesterol depletion, achieved by growing cells in lipoprotein-deficient serum, increases Na–P_i cotransport activity and the abundance of apical membrane and total cellular NaPi-IIa protein. Chronic cholesterol depletion also increases membrane lipid fluidity and alters lipid microdomains as determined by Laurdan fluorescence spectroscopy. Chronic cholesterol enrichment, achieved by LDL loading, decreases Na–P_i cotransport

activity and the abundance of apical membrane and total cellular NaPi-IIa protein. Hence, acute and chronic alterations in cholesterol content modulate Na–P_i cotransport activity in OK cells through mechanisms that include interactions of NaPi-IIa with lipid microdomains and the regulation of apical BBM NaPi-IIa protein abundance, supporting in vivo observations of the changes that occur in the ageing kidney[144].

Studies involving glucocorticoid treatment in mice have revealed additional contributions of BBM lipids to the regulation of Na–P_i cotransport activity. Administration of dexamethasone to rats decreases the maximal velocity of Na–P_i cotransport paralleled by decreases in the abundance of NaPi-IIa mRNA and protein and an increase in BBM glucosylceramide content. Reducing BBM glucosylceramide content induces an increase in Na–P_i cotransport activity and BBM NaPi-IIa protein abundance[56], suggesting that the inhibitory effect of dexamethasone on Na–P_i cotransport activity might be mediated by an increase in BBM glucosylceramide content[56].

Dietary K^+ deficiency also increases BBM glucosylceramide content[26]. As discussed earlier, K^+ deficiency increases urinary P_i excretion and decreases the maximal velocity of BBM NaPi cotransport activity. Surprisingly, the decrease in Na–P_i cotransport activity occurs despite an increased abundance of NaPi-IIa protein at the BBM[26]. Of note, the decrease in Na–P_i transport in response to K^+ deficiency is paralleled by alterations in the lipid composition of the BBM, characterized by increases in sphingomyelin, glucosylceramide and ganglioside GM3 content and a decrease in BBM lipid fluidity. Inhibition of glucosylceramide synthesis increases BBM Na–P_i cotransport activity in control and in K^+-deficient rats. These changes in transport activity occur independently of changes in BBM NaPi-IIa protein or renal cortical *Slc34a1* mRNA abundance, suggesting that K^+ deficiency in rats inhibits renal Na–P_i cotransport activity through post-translational mechanisms that are mediated in part by alterations in glucosylceramide content and membrane lipid dynamics[26].

Further studies have investigated the molecular mechanisms by which BBM lipids regulate Na–P_i cotransport activity. Fluorescence spectroscopy and multiphoton excitation (MPE) fluorescence microscopy using the lipid probe Laurdan have revealed the presence of dynamic membrane microdomains, known as lipid rafts in the BBM[146,147,148,149]. Scanning fluorescence correlation spectroscopy (SFCS) studies[150] show that in response to K^+ deficiency, NaPi-IIa partitions in microdomains of the apical BBM that are enriched for cholesterol, sphingomyelin and glycosphingolipids and that the increased presence of NaPi-IIa in these microdomains decreases the activity of the transporter. Importantly, these studies also demonstrated that localization of NaPi-IIa in these lipid rafts is associated with decreased lateral diffusion of the transporter within the BBM and the formation of NaPi-IIa pentamers rather than dimers, which is correlated with decreased transport activity[27] (Fig. 3).

Clinical consequences of mutations

Renal P_i losses occur in several systemic syndromes, such as those involving generalized inherited or acquired dysfunction of the proximal tubule (for example, Fanconi syndrome) and those caused by inherited disorders that specifically affect renal and extrarenal P_i regulation. Renal P_i wasting is caused by inactivating mutations in *SLC34A1* and *SLC34A3*, which directly reduce renal P_i reabsorption, causing nephrocalcinosis and kidney stones.

SLC34A1

Several genome-wide association studies (GWAS) have linked single-nucleotide polymorphisms in or next to *SLC34A1* to serum levels of P_i (ref.[151]), calcium-phosphate kidney stones[152], hypophosphataemia and low PTH[153].

Mutations in *SLC34A1* have been identified in adult patients with kidney stones and reduced bone density[154], in children with hypophosphataemia and hyperphosphaturia[155] and in children with infantile idiopathic hypercalciuria[156] or with nephrocalcinosis and kidney stones[153,157,158,159,160,161]. Patients from one large family with *SLC34A1* mutations also showed signs of proximal tubular dysfunction[160]. Some studies have also identified associations between *SLC34A1* mutations and metabolic acidosis or epilepsy, sensorineural deafness and learning deficiencies[162], although these manifestations might not be directly linked to mutations in *SLC34A1*. Larger deletions encompassing *SLC34A1* are found in patients with Sotos syndrome, which is characterized by learning deficiencies, facial dysmorphia, overgrowth, hypercalcaemia and nephrocalcinosis[163]. Unless renal manifestations develop into CKD, the clinical symptoms of patients with *SLC34A1* mutations seem to improve as they enter adulthood.

To date, 29 mutated sites have been identified in *SLC34A1*; most of these result in missense mutations, small in-frame deletions, frameshifts or early stop codons[153,154,155,157,158,159,160,161,164]. More than half of these mutations affect residues located within the highly predicted conserved transmembrane domains of the transporter. Functional studies show that several of these mutants have reduced transporter function mostly owing to trafficking defects and intracellular retention of the transporter[156,159,165]. One mutation — an in-frame deletion of seven amino acids at the cytoplasmic amino-terminal tail (91del7) — has been detected in several patients either in compound heterozygosity or in homozygosity. The clinical features of patients with this mutation are similar to those of patients carrying other *SLC34A1* mutations (nephrocalcinosis, hypercalcaemia and hyperphosphataemia)[156], suggesting that the 91del7 mutation is pathogenic. Functional studies show no or only a mild transport defect[166]; however, expression of the mutant transporter at the apical membrane is lower than that of wild-type protein, with some intracellular accumulation, together suggesting a possible trafficking defect[156]. Notably, genetic databases such as the Exome Aggregation Consortium browser show that this mutation has a high minor allele frequency of 0.018, which suggests that nearly 2% of the general population is heterozygous for this mutation. This frequency is comparable to the combined allele frequency of all proven pathogenic exonic mutations, which is 0.022; the total allele frequency of all nucleotide changes that lead to an altered amino acid sequence is 0.07. Because the impact of carrying only one allele with the 91del7 mutation or other

mutations is unclear, further clinical studies and mechanistic tests are required. Nevertheless, some of the mutations might be associated with a higher risk of developing calcium-phosphate kidney stones in adulthood. A genetic study of Pakistani families with kidney stones found heterozygous mutations in *SLC34A1* in several families, which affected the transport activity of the transporter[165]. Moreover, heterozygous *SLC34A1* mutations were found in three French patients with kidney stones[154].

Most *SLC34A1* mutations are homozygous or compound heterozygous with an autosomal recessive inheritance of clinical symptoms. The existence of family members carrying mutant forms of *SLC34A1* but with no clinical abnormalities suggests that one mutated allele is not sufficient for disease manifestations to occur. This observation is somewhat in contrast to the above-described analyses of 91del7 allele frequencies, which suggest a link between heterozygous 91del7 mutations and the presence of calcium-phosphate stones on the basis of the identification of these and similar mutations in cohorts of patients with kidney stone disease. Whether this association exists by chance, given that the minor allele frequency of *SLC34A1* mutations is high and that up to 10% of the population suffers at least from one stone episode during their lifetime, remains to be clarified. Available data suggest that the link between monoallelic *SLC34A1* mutations and stone disease risk is complex. In one study, three adult patients who presented with calcium-phosphate stones and reduced bone density had only one mutated *SLC34A1* allele[154]. By contrast, in another study, heterozygous family members of patients with calcium-phosphate stones and homozygous mutations in *SLC34A1* did not show a higher frequency of kidney stones than that of the general population[155]. Nevertheless, available GWAS clearly support an association of *SLC34A1* with stone disease[153]. Because NaPi-IIa forms homodimers[27,141] in which both subunits function independently[167], monoallelic mutations could impair the trafficking of NaPi-IIa dimers comprising wild-type and mutant proteins, thereby causing a dominant negative effect. Alternatively, the function of one normal allele may not be sufficient to adapt renal P_i handling to changing metabolic and dietary demands, thereby increasing a carrier's risk of developing kidney stones.

In mice, ablation of *Slc34a1* causes hypophosphataemia resulting from urinary P_i loss and is associated with low PTH and FGF23 and higher than normal $1,25(OH)_2D_3$ levels[50,156]. NaPi-IIa-deficient mice develop renal calcifications containing calcium phosphate and calcium oxalate when fed diets high in P_i or oxalate[168,169]. Similar to human patients with biallelic *SLC34A1* mutations, NaPi-IIa-deficient mice are also hypercalciuric[50,156]. Urinary P_i wasting in this context stimulates $1,25(OH)_2D_3$ synthesis and inhibits $1,25(OH)_2D_3$ degradation. High levels of $1,25(OH)_2D_3$ stimulate intestinal Ca^{2+} absorption, which promotes nephrolithiasis and calcinosis. Of note, the renal calcifications of NaPi-IIa-deficient mice can be reduced by restricting $1,25(OH)_2D_3$ availability and supplementing P_i levels[170]. Children with homozygous or compound heterozygous mutations in *SLC34A1* can improve plasma calcium and phosphate levels and growth with P_i supplementation whereas vitamin D_3 supplementation can be detrimental[156]. Of major interest for the adult population is the possibility of gene–diet interactions, whereby the combination of monoallelic mutations with specific P_i, Ca^{2+}, oxalate and vitamin D_3 exposures might trigger nephrolithiasis.

SLC34A3

Biallelic mutations in *SLC34A3* cause hereditary hypophosphataemic rickets with hypercalciuria (HHRH)[171,172,173] (reviewed elsewhere[174]). Although these patients also manifest with hypophosphataemia, hyperphosphaturia, hypercalciuria and elevated $1,25(OH)_2D_3$ levels, they can be distinguished from patients carrying *SLC34A1* mutations on the basis of their higher risk of rickets. Nearly all patients with HHRH develop kidney stones or nephrocalcinosis. Clinical problems often persist into adulthood, suggesting that in humans, the contribution of NaPi-IIa is higher in earlier phases of life whereas NaPi-IIc might be more important in the adult kidney, although long-term follow-up of patients with *SLC34A1* and *SLC34A3* mutations are needed to address this possibility. The exact contribution of both transporters to age-dependent renal P_i handling also requires clarification.

To date, 34 mutations have been identified in *SLC34A3* (refs[171,172,173,174]); most of these mutations are missense, alter potential splice sites or generate premature stop codons. Only few mutations have been characterized in any detail, and these were found to cause retention of NaPi-IIc in the endoplasmic reticulum, reduce its stability at the plasma membrane or reduce its transport activity[174]. According to the ExAC database, pathogenic mutations in *SLC34A3* (with a minor allele frequency of 0.002) are around ten times less frequent than pathogenic mutations in *SLC34A1*. When suspected pathogenic mutations are included in these analyses, the total allele frequency of pathogenic mutations in *SLC34A3* increases to 1.5%, but this increase is mostly due to two very frequent allele variants that have an allele frequency of nearly 0.4% and 0.8%. The relevance of these variants in terms of NaPi-IIc activity is, however, unclear and requires detailed analyses.

Two mouse models have been generated with constitutive or renal-specific and inducible depletion of *Slc34a3*. Both models show normal growth, normal renal P_i handling with normophosphataemia and normal bone growth and morphology[175,176]. Whereas constitutive depletion results in hypercalcaemia with hypercalciuria, high levels of $1,25(OH)_2D_3$ and low FGF23 (ref.[175]), mice with inducible deletion of renal *Slc34a3* had similar Ca^{2+} levels in plasma and urine as well as normal $1,25(OH)_2D_3$ and FGF23. No evidence for compensation by other renal P_i transporters, that is, NaPi-IIa or PIT2, was found[176], suggesting that in adult murine kidney NaPi-IIc is dispensable and that mice are not a good model for HHRH.

SLC34A2

Biallelic mutations in *SLC34A2* have been identified in patients with pulmonary alveolar microlithiasis (PAM), which is characterized by progressive deposition of calcium-phosphate microcrystals in the lung, subsequent tissue destruction, pulmonary fibrosis and insufficiency and in some patients cor pulmonale[177,178,179]. Heterozygous mutations have also been linked to testicular microlithiasis in a few patients[177], but this association is yet to be confirmed by independent studies. Twenty mutations have thus far been reported, comprising deletions, frameshifts and missense mutations as well as mutations that induce changes in potential splice sites and the promoter region[177,178,179], although the functional consequences of these mutations on transport activity, trafficking or protein stability have not been well

characterized. One study demonstrated that at least two truncated *SLC34A2* mutants do not transport P_i when expressed in *Xenopus* oocytes[179].

Despite prominent expression of NaPi-IIb in intestine, patients with *SLC34A2* mutations have no known phenotype related to intestinal P_i absorption or systemic P_i homeostasis. In addition to its expression in the intestine, NaPi-IIb is also expressed in type II pneumocytes in the lung[180] — cells that are important for surfactant production. A study that expressed one *SLC34A2* variant in an alveolar cell line demonstrated that P_i transport was diminished, suggesting that NaPi-IIb could have a role in controlling extracellular P_i levels in alveolar fluid[181].

Mice with *Slc34a3* deletion have been generated, mainly to characterize the role of NaPi-IIb in intestine[182,183]. These models indicate that NaPi-IIb is the main NaPi-II cotransporter in the ileum, although depletion of *Slc34a3* has only mild consequences on P_i and hormonal levels[182,183]. Mice with deletion of *Slc34a3* specifically in lung epithelium have increased P_i levels in their bronchoalveolar fluid, together with calcium-phosphate microcrystals, invasion of macrophages and signs of inflammation and fibrosis[184]. The microcrystals could be resolved by bronchoalveolar lavage or by feeding mice with a low-P_i diet for 4 weeks. Whether these experimental therapies are relevant for human patients remains to be shown.

Mechanism of epithelial P_i transport

Our current understanding of the transport mechanisms and structure–function relationships of NaPi-II transporters has come largely from overexpression studies in *X. laevis* oocytes and the use of voltage clamp, fluorometry and tracer uptake assays. This approach has facilitated the characterization of a homogeneous population of transporters without contamination from other transmembrane P_i influx pathways as can occur when renal or intestinal tissue is used.

Energetics and kinetics

All three NaPi-II isoforms are Na^+-dependent and preferentially transport divalent P_i (HPO_4^{2-}); however, a key difference between the isoforms is found for NaPi-IIc[8]: NaPi-IIa and NaPi-IIb are electrogenic[7,185] whereas NaPi-IIc is electroneutral[8]. A strict stoichiometric relationship exists between Na^+ and P_i in NaPi-II-mediated transport: this ratio is 3:1 for the electrogenic isoforms, resulting in one net positive charge transported per cycle[186], and 2:1 for NaPi-IIc, resulting in zero net charge movement[8,187]. Thus, the uphill movement of anionic P_i is driven by the electrochemical gradient provided by Na^+ ions. This gradient is maintained in native cells by the Na^+/K^+-ATPase that is highly abundant at the basolateral membrane. The physiological basis for having both electrogenic and electroneutral isoforms expressed in the same organ is not known.

Detailed investigations of the transport properties of the NaPi-II proteins have culminated in a kinetic model for NaPi-II-mediated transport[188]. This model depicts P_i transport at the single-molecule level as a cyclic process, comprising a sequence of transitions between conformationally distinct states of the protein (Fig. 4a). When the empty transporter is in its outward-facing conformation (state 1), two external Na^+ ions

bind sequentially to allow P_i access to the binding site within the carrier (states 2–4). A third Na^+ ion then binds (state 5) and a translocation event occurs (state 6), allowing release of the substrates into the cytosol (state 7 followed by state 0). For NaPi-IIa and NaPi-IIb, the rate of return of the empty carrier from state 0 to state 1 is dependent on the membrane potential, which results from the movement of charges intrinsic to the protein that are displaced by the transmembrane electric field. The release of the third Na^+ ion into the cytosol is also thought to involve a small charge displacement[189]. The charge movements that are thought to reflect these conformational changes are small, amounting to an effective charge of one electron per transport cycle per protein, and can be detected only by analysing a large population of independent proteins. The charge movements manifest as pre-steady-state current relaxations as the transporters respond to rapid changes in membrane potential (Fig. 4b). Similar to the gating charges of ion channels, they display properties of nonlinear capacitive currents[190]. When Na^+ ions are present in the extracellular medium, the displacement charge is increased (Fig. 4c), indicating that an additional movement of charge accompanies the molecular rearrangements when Na^+ ions bind. These conformational changes have been indirectly measured by means of voltage clamp fluorometry (VCF)[188]. When both Na^+ and P_i are present, the translocation from outward-facing (state 4) to inward-facing (state 5) conformations is an electroneutral process. Thus, it is the release of the final Na^+ ion that gives rise to the transport-related P_i-dependent current (I_{Pi}) (Fig. 4d). This current is an indirect measure of the P_i transport rate, assuming invariant driving force and number of active transporters. The voltage dependence of P_i transport in the steady state can be fully accounted for by the voltage-dependent kinetics of the empty carrier and steps involving cation binding and release. Transport turnover rates based on biophysical measurements are estimated to be $<10\ s^{-1}$ at ~20 °C, and the rate-limiting step in the transport cycle is thought to be the translocation of the fully loaded carrier. The transport cycle of electroneutral NaPi-IIc is essentially the same as for NaPi-IIa and NaPi-IIb, except that the first Na^+ ion to bind is not translocated and has been hypothesized to act as a catalytic activator[191]. Importantly, neither pre-steady-state relaxations nor steady-state P_i-dependent currents are detectable for this isoform, consistent with its electroneutrality[8,187,191]. The molecular basis for electrogenicity has been identified and rests on three critical amino acids located deep in the transport domain (Fig. 5), one of which is charged in all electrogenic isoforms[187] (D224; Fig. 5a). The absence of this charge in NaPi-IIc may prevent the translocation of the first Na^+ ion[192].

Investigations of transporter function have also assessed substrates other than Na^+ and P_i. Transport by all isoforms is reduced by acidification of the external medium. This reduction is in part due to titration of P_i, which reduces the availability of divalent P_i but also arises because protons modulate the kinetics of the empty carrier and effectively compete with the final Na^+ interaction[193,194,195]. Use of lithium ions as a cationic probe showed that a Li^+ ion competes with Na^+ for occupancy at the first cation binding site. For the electrogenic NaPi-IIb, one Li^+ ion can substitute for one of the three Na^+ ions transported[196,197].

Structure–function relationships

On the basis of biochemical assays, freeze fracture studies[198] and assessment of the structurally similar dicarboxylate cotransporter, VcINDY[199], it is likely that NaPi-II proteins assemble in the membrane as dimers, although each protomer is functionally

independent[200]. A 3D crystal structure of NaPi-II proteins or their bacterial homologues does not currently exist; however, homology modelling studies[192,201] suggest that they may have a 3D architecture similar to that of dimeric VcINDY[199], which is a member of the divalent anion/Na^+ symporter (DASS) family. Homology modelling using VcINDY as a template has enabled prediction of residues involved in substrate coordination — predictions that have been confirmed by analysing the functional consequences of single point mutations at these sites[192,201]. The secondary topology of VcINDY is characterized by two inverted repeat units in which each repeated unit contributes to the transport and oligomerization domains[201] (Fig. 5a). This structure is expected to be common to all three NaPi-II isoforms as well as their bacterial homologues, consistent with the similarity of their hydrophobicity profiles[202]. Each repeated unit contains stretches of high sequence similarity, and these are predicted to undergo conformational changes during transport and to allow substrate accessibility from either side of the membrane[202], consistent with the alternating access model for carrier-mediated membrane transport in which, depending on the state of occupancy, substrates can access their binding sites from either the external or internal media but not simultaneously[203].

Structure–function studies combined bioinformatics and functional assays using the substituted cysteine accessibility (SCAM) technique, crosslinking, chimaeras containing complementary elements from NaPi-IIa and NaPi-IIb and site-directed mutagenesis to identify functionally important regions[188]. An inward-facing conformation was predicted using the repeat swap strategy previously applied to study other carrier proteins, including VcINDY[199,204]. Comparison of the outward and inward conformations suggests that similar to the SLC14 family, SLC34 (NaPi-II) proteins most likely mediate transport using the so-called ‘elevator mechanism’, which involves an ~37° rotation and 15 Å vertical displacement of the transport domain relative to the oligomeric interface domain that acts as a fixed scaffold[205] (Fig. 5b). This mechanism allows substrates to bind in the outward-facing conformation but does not allow them direct access to the cytosol; when fully loaded, the transport domain then translocates the substrates by changing to the inward-facing conformation, whereupon the substrates are released to the cytosol. The relatively large movements predicted by this model have been detected by VCF[188].

Substrates and inhibitors of NaPi

To date, only two substrates for NaPi transporters — P_i and arsenate — and only a handful of competitive inhibitors have been described. The known inhibitors can be used to study the characteristics of the P_i transporters and to inhibit their function for therapeutic purposes. Some inhibitors are competitive and bind to the same binding site as P_i; others are non-competitive and bind in non-P_i-binding parts of the transporters[206]. Here, we focus on the better known and available inhibitors. A more complete list can be obtained elsewhere[206].

Phosphonoformic acid

Phosphonoformic acid (PFA) is the most commonly used competitive inhibitor of P_i transport and is also a potent antiviral drug (foscarnet). PFA is structurally very similar to P_i (Fig. 6); extending its formate side chain attenuates its inhibitory properties[207]. PFA inhibits P_i transport in rat kidney and jejunum BBMVs with K_i values of 0.46 mM

and 0.37 mM, respectively[208]. The K_i values for PFA inhibition of rat NaPi-IIa, NaPi-IIb and NaPi-IIc expressed in *X. laevis* were 0.7–1 mM, 0.16 mM and 0.9 mM, respectively[208]. PFA is, however, a very poor inhibitor of PIT1 and PIT2 (ref.[209]). Binding of PFA to NaPi-IIa also prevents P_i-induced currents and Na^+ slippage (that is, Na^+ binding and then leakage inside the cell causing a conductivity rise) at low P_i concentration[210].

Administration of PFA either parenterally[207,211] or orally[212] to rats induces phosphaturia, although the effect on phosphataemia is variable. However, the nephrotoxicity of PFA impedes its use in patients with CKD-related hyperphosphataemia[213].

Arsenate

Arsenate is also structurally very similar to P_i and is a competitive inhibitor of the NaPi members. The affinity of arsenate for NaPi transporters is lower than that of P_i (ref.[131]), exemplified by the finding that the arsenate K_i values in kidney[3] and small intestine[2] BBMVs are higher than the K_m for P_i transport. Arsenate also mimics P_i most likely and interacts with an intracellular P_i sensor in OK kidney cells[214].

NAD

NAD and its precursor niacin (vitamin B_3) also inhibit P_i transport, but the mechanism of inhibition is unclear. In vitro studies in renal[215] and intestinal[216] BBMVs suggest that NAD competitively inhibits P_i transport, whereas evidence from in vivo studies suggests a non-competitive mechanism[215]. Nicotinamide and its analogues increased the cAMP content in proximal tubule suspensions by 2–5-fold[205], but this increase was not confirmed in rats in vivo[206]. NAD induces phosphaturia within 1 h of intraperitoneal administration even in animals deprived of dietary P_i (ref.[217]). An analysis of rats with hepatectomy-induced hypophosphataemia and hyperphosphaturia showed upregulation of renal nicotinamide phosphoribosyltransferase (Nampt), the rate-limiting enzyme in NAD biosynthesis, which was accompanied by downregulation of NaPi-IIa and NaPi-IIc expression in the proximal tubule[218]. The same researchers also demonstrated a role for Nampt and NAD in regulating circadian variations in P_i levels by mediating changes in NaPi-IIa and NaPi-IIc abundance[219].

Tenapanor

Tenapanor was initially designed as an inhibitor of the intestinal sodium–hydrogen exchanger NHE3 but was subsequently found to inhibit intestinal absorption of P_i in healthy and nephrectomized rats, attenuating ectopic calcification and hyperphosphataemia[220]. Tenapanor does not, however, inhibit P_i transport. Rather, inhibition of NHE3 modulates intestinal tight junctions, leading to increased transepithelial electrical resistance, which reduces the paracellular absorption of P_i (ref.[221]).

PF-06869206

PF-06869206 is an azaindole analogue and a new selective inhibitor of NaPi-IIa developed by Pfizer[222]. It has an IC_{50} of 0.4 μM when administered to HEK293 cells

that express rat or mouse NaPi-IIa and is a poor inhibitor of other P_i transporters. In rats, the bioavailability of this drug is very high, but both rats and mice show moderate clearance, which is saturated at high drug concentration. The role of PF-06869206 in CKD is, however, questionable, because P_i transport and reabsorption are already inhibited by high FGF23 plasma concentrations and by PTH, and intestinal absorption of P_i remains highly functional[223].

JTP-59557

The triazole derivative JTP-59557 from Japan Tobacco Inc. was shown to be a non-competitive inhibitor of intestinal P_i transport in rat BBMVs with a reported IC_{50} <1 μM, and of intestinal absorption ex vivo[224]. The effects on other P_i transporters is unknown, as is the pharmacokinetic behaviour or toxicity.

ASP3325

Conflicting results have been reported with use of the chemical ASP3325 (Astellas Pharma Inc.) in rats and humans. This drug inhibits rat NaPi-IIb with an IC_{50} of 88 nM, inhibiting intestinal P_i absorption, and improves P_i renal excretion and experimental hyperphosphataemia. These benefits have not, however, been observed in human patients with hyperphosphataemia[225].

Conclusions

Over the past quarter century, tremendous progress has been made in our understanding of the regulation of NaPi-IIa, NaPi-IIb and NaPi-IIc and their critical role in maintaining P_i homeostasis. However, despite this progress, more work is needed to determine the mechanisms underlying the differential regulation of these transporters in health and disease, particularly in CKD. In addition, the exact mechanisms involved in the regulation of intestinal P_i reabsorption also remain an enigma. Greater understanding of the molecular mechanisms underlying P_i transport and its regulation is likely to lead to the development of additional approaches to target specific transporters, which will lead to new treatments for maintaining P_i homeostasis and for the prevention of the life-threatening complications associated with P_i dysregulation.

Figure legends

Figure 1
Trafficking of the Na^+-dependent inorganic phosphate (P_i) cotransporters NaPi-IIa and NaPi-IIc to and from the brush-border membrane (BBM) of kidney tubular epithelial cells occurs through interaction of the transporters with PDZ domain-containing proteins, such as sodium–hydrogen antiporter 3 regulating factor 1 (NHERF1) and NHERF3. The two renal NaPi transporters interact with the NHERF proteins with different affinities: NaPi-IIa has a higher affinity for NHERF1 whereas NaPi-IIc has a higher affinity for NHERF3. Parathyroid hormone (PTH) downregulates the expression of NaPi-IIa. Binding of PTH to receptors on the basolateral membrane of renal proximal tubules preferentially activates adenylyl cyclase (AC)–protein kinase A (PKA)-dependent pathways, whereas binding of PTH to apical receptors results in preferential activation of phospholipase C (PLC)–protein kinase C (PKC)-dependent signalling. This differential activation is due to the capacity of NHERF1, expressed specifically in the apical BBM, to form a complex with PLC, thus resulting in activation of PKC. PKA and PKC signalling converges, at least partially, on extracellular-signal regulated kinases (ERKs). Activation of these kinases results in phosphorylation of NHERF1, thereby reducing the affinity of NHERF1 for NaPi-IIa and resulting in release of the cotransporter from its anchoring partner. Upon disassembly, NaPi-IIa is endocytosed and finally targeted to lysosomes where it is degraded. PTH also induces the internalization of NaPi-IIc, but the fate and recycling of this transporter are not completely understood. Internalization of both cotransporters depends on myosin VI, a minus-end-directed actin motor protein. Microscopy studies of transfected opossum kidney cells show that PTH induces more rapid internalization of NaPi-IIa and increased diffusion of NaPi-IIa compared with NaPi-IIc. Similar time course differences in internalization of NaPi-IIa and NaPi-IIc also occur in mice treated with PTH. PtdIns(4,5)P_2, phosphatidylinositol 4,5-bisphosphate; PTHR1, parathyroid hormone 1 receptor.

Figure 2
a | Several PDZ domain-containing proteins exist. Sodium–hydrogen antiporter 3 regulating factor 1 (NHERF1) and NHERF2 consist of two PDZ domains and an ezrin-radixin-moesin-binding domain (ERM-BD), which enables the protein to anchor to the actin-based cytoskeleton. NHERF3 and NHERF4 contain four PDZ domains but lack the ERM-BD. SHANK2E contains several motifs that mediate protein–protein interaction, including ankyrin repeats (AR), an SH3 domain, a PDZ domain, a proline-rich region (PR) and a sterile α-motif (αS). The AR interacts with the α-subunit of spectrin, an actin-binding protein. CFTR-associated ligand (CAL) consists of two coil-coil domains (CC) and a single PDZ domain. PDZ domains that interact with NaPi transporters are indicated by asterisks. **b** | NHERF1, NHERF3 and SHANK2E are associated with the brush-border membrane, whereas NHERF2 and NHERF3 are expressed in subapical vesicles and CAL is expressed in the *trans*-Golgi network. NaPi, Na^+-dependent inorganic phosphate cotransporter.

Figure 3
Na^+-dependent inorganic phosphate (P_i) cotransporter NaPi-IIa is present in the apical brush-border membrane of tubule epithelial cells as a dimer, where it acts as a cotransporter for Na^+ and divalent P_i (HPO_4^{2-}). Saturation of lipid membrane microdomains, for example, with ageing or cholesterol loading, leads to the formation of lipid rafts, which are characterized by increased concentrations of cholesterol and glycosphingolipids within the membrane. NaPi-IIa within these lipid rafts forms pentamers, which have slower diffusion and impaired P_i transport activity.

Figure 4
a | A kinetic model is shown for the electrogenic isoforms (Na^+-dependent inorganic phosphate

(P_i) cotransporters NaPi-IIa and NaPi-IIb). The cotransport cycle comprises transitions between a series of conformations (stages 0–7) that are linked kinetically by partial reactions (arrows). Three partial reactions (red) are voltage-dependent and involve charge displacements within the transmembrane electric field. All other partial reactions are electroneutral (black arrows). For the normal, physiologically relevant cotransport cycle, two Na^+ ions bind sequentially to the outward-facing empty carrier (state 0), leading to a conformational (state 3) that allows P_i binding and a third Na^+ ion to bind, leading to the fully loaded carrier. A translocation event takes place (states 4–5) and substrates are subsequently released (state 0), whereupon the cycle returns to state 1. The displacement of the empty carrier intrinsic charge (under the influence of the transmembrane electric field) and charge associated with the initial Na^+ ion interactions can fully account for the observed voltage dependence of the electrogenic NaPi-IIa and/or NaPi-IIb. In the absence of P_i, Na^+ ions can 'leak' through the transporter at a low rate (states 2–6)[210,226]. The order in which substrates are released into the cytosol has not been fully determined (indicated by dashed arrows), and the charge contribution from the internal Na^+ binding transition is small. For the electroneutral NaPi-IIc, the transport cycle is similar but the first Na^+ ion is not transported, and it is electrically silent. **b–d** | Using experimental manipulations, three unique electrogenic responses have been resolved. **b** | Pre-steady-state current relaxations reflect the empty carrier reorientation from inward-facing to outward-facing conformations. **c** | When Na^+ ions are present in the extracellular medium, the displacement charge is increased, indicating an additional movement of charge. **d** | When both Na and P_i are present, the transporter is mostly in the cotransport mode and the relaxations are strongly suppressed. The release of the final Na^+ ion gives rise to the transport-related P_i-dependent current (I_{Pi}).

Figure 5

a | Secondary topology of Na^+-dependent inorganic phosphate (P_i) cotransporter NaPi-II based on homology modelling using the dicarboxylate transporter VcINDY as a template[201]. Two repeat units (RU1 and RU2) contain a number of duplicated amino acids (not shown). Rectangular blocks represent α-helical stretches. Transmembrane domains 7 and 8, the large extracellular loop linking the two repeat units and amino and carboxyl termini, were not included in the homology model. The transport domain regions are coloured orange and the oligomerization (scaffold) domain is coloured mauve. Numbering is according to human NaPi-IIa. The two hairpin loops (HP_{1a} and HP_{1b}, and HP_2 and HP_{2b}) are proposed to be involved in coordination of the second and third Na^+ ions and P_i together with the linkers L2ab and L5ab. The three amino acids critical for conferring voltage electrogenicity (A218, A220 and D224) at the cytosolic end of TM3 are indicated. **b** | A 3D model of NaPi-IIb (flounder isoform) in two conformations illustrates how the proposed elevator transport mechanism operates[205]. Only one protomer is shown. The scaffold domains of each protomer (shown in purple) would abut one another to stabilize the dimeric structure and allow independent movement of the transport domains. In the outward conformation site, Na1 is occupied first, followed by Na2, P_i and Na3. The inward conformation is reached by vertical displacement and partial rotation of the transport domain to allow release of substrates to the cytosol.

Figure 6

A comparison of the 2D molecular structures of known competitive inhibitors (arsenate and phosphonoformic acid (PFA)) shows the structural similarity with inorganic phosphate (P_i). Na^+-dependent P_i cotransporter NaPi-II can be inhibited by competitive inhibitors, which bind to the same binding site as P_i (represented by (1); for example, PFA and arsenate), and non-competitive inhibitors, which bind to non-P_i-binding sites (represented by (2); for example, triazoles and azaindoles). Inhibition of P_i transport can also be achieved by interfering with the interaction of P_i transporters with PDZ proteins and inducing rearrangements of the transporters and associated proteins in the plasma membrane (3). NAD has been reported to have both competitive and non-competitive inhibitor properties and, in vitro, increases the intracellular concentration of cAMP, which could potentially inhibit P_i transport (4). Tenapanor (not shown) acts by indirect mechanisms, possibly by modulating intestinal

epithelial tight junctions through its actions on intestinal sodium–hydrogen exchanger NHE3, leading to increased transepithelial electrical resistance and reduced paracellular P_i absorption.

References

1. Baumann, K., de Rouffignac, C., Roinel, N., Rumrich, G. & Ullrich, K. J. Renal phosphate transport: inhomogeneity of local proximal transport rates and sodium dependence. *Pflugers Arch.* **356**, 287–298 (1975).
2. Berner, W., Kinne, R. & Murer, H. Phosphate transport into brush-border membrane vesicles isolated from rat small intestine. *Biochem. J.* **160**, 467–474 (1976).
3. Hoffmann, N., Thees, M. & Kinne, R. Phosphate transport by isolated renal brush border vesicles. *Pflugers Arch.* **362**, 147–156 (1976).
4. Ullrich, K. J., Rumrich, G. & Kloss, S. Phosphate transport in the proximal convolution of the rat kidney. I. Tubular heterogeneity, effect of parathyroid hormone in acute and chronic parathyroidectomized animals and effect of phosphate diet. *Pflugers Arch.* **372**, 269–274 (1977).
5. Ullrich, K. J., Rumrich, G. & Kloss, S. Phosphate transport in the proximal convolution of the rat kidney II. Effect of extracellular Ca^{2+} and application of the Ca^{2+} ionophore A 23187 in chronic PTX animals. *Pflugers Arch.* **375**, 97–103 (1978).
6. Magagnin, S. et al. Expression cloning of human and rat renal cortex Na/P_i cotransport. *Proc. Natl Acad. Sci. USA* **90**, 5979–5983 (1993).
7. Hilfiker, H. et al. Characterization of a murine type II sodium-phosphate cotransporter expressed in mammalian small intestine. *Proc. Natl Acad. Sci. USA* **95**, 14564–14569 (1998).
8. Segawa, H. et al. Growth-related renal type II Na/Pi cotransporter. *J. Biol. Chem.* **277**, 19665–19672 (2002).
9. Segawa, H. et al. Npt2a and Npt2c in mice play distinct and synergistic roles in inorganic phosphate metabolism and skeletal development. *Am. J. Physiol. Renal Physiol.* **297**, F671–F678 (2009).
10. Tenenhouse, H. S. & Beck, L. Renal Na^+-phosphate cotransporter gene expression in X-linked Hyp and Gy mice. *Kidney Int.* **49**, 1027–1032 (1996).
11. Lederer, E. & Miyamoto, K. Clinical consequences of mutations in sodium phosphate cotransporters. *Clin. J. Am. Soc. Nephrol.* **7**, 1179–1187 (2012).
12. Forster, I. C., Hernando, N., Biber, J. & Murer, H. Phosphate transporters of the SLC20 and SLC34 families. *Mol. Aspects Med.* **34**, 386–395 (2013).
13. Levi, M. et al. Cellular mechanisms of acute and chronic adaptation of rat renal P(i) transporter to alterations in dietary P(i). *Am. J. Physiol.* **267**, F900–F908 (1994).
14. Villa-Bellosta, R. et al. The Na^+-Pi cotransporter PiT-2 (SLC20A2) is expressed in the apical membrane of rat renal proximal tubules and regulated by dietary Pi. *Am. J. Physiol. Renal Physiol.* **296**, F691–F699 (2009).
15. Pfister, M. F. et al. Cellular mechanisms involved in the acute adaptation of OK cell Na/Pi-cotransport to high- or low-Pi medium. *Pflugers Arch.* **435**, 713–719 (1998).
16. Segawa, H. et al. Internalization of renal type IIc Na-Pi cotransporter in response to a high-phosphate diet. *Am. J. Physiol. Renal Physiol.* **288**, F587–F596 (2005).
17. Lotscher, M., Kaissling, B., Biber, J., Murer, H. & Levi, M. Role of microtubules in the rapid regulation of renal phosphate transport in response to acute alterations in dietary phosphate content. *J. Clin. Invest.* **99**, 1302–1312 (1997).
18. Madjdpour, C., Bacic, D., Kaissling, B., Murer, H. & Biber, J. Segment-specific expression of sodium-phosphate cotransporters NaPi-IIa and -IIc and interacting proteins in mouse renal proximal tubules. *Pflugers Arch.* **448**, 402–410 (2004).

19. Weinman, E. J. et al. Parathyroid hormone inhibits renal phosphate transport by phosphorylation of serine 77 of sodium-hydrogen exchanger regulatory factor-1. *J. Clin. Invest.* **117**, 3412–3420 (2007).
20. Shenolikar, S., Voltz, J. W., Minkoff, C. M., Wade, J. B. & Weinman, E. J. Targeted disruption of the mouse NHERF-1 gene promotes internalization of proximal tubule sodium-phosphate cotransporter type IIa and renal phosphate wasting. *Proc. Natl Acad. Sci. USA* **99**, 11470–11475 (2002).
21. Capuano, P. et al. Expression and regulation of the renal Na/phosphate cotransporter NaPi-IIa in a mouse model deficient for the PDZ protein PDZK1. *Pflugers Arch.* **449**, 392–402 (2005).
22. Ritthaler, T. et al. Effects of phosphate intake on distribution of type II Na/Pi cotransporter mRNA in rat kidney. *Kidney Int.* **55**, 976–983 (1999).
23. Biber, J., Hernando, N. & Forster, I. Phosphate transporters and their function. *Annu. Rev. Physiol.* **75**, 535–550 (2013).
24. Bergwitz, C. & Juppner, H. Regulation of phosphate homeostasis by PTH, vitamin D, and FGF23. *Annu. Rev. Med.* **61**, 91–104 (2010).
25. Thomas, L. et al. Acute adaption to oral or intravenous phosphate requires parathyroid hormone. *J. Am. Soc. Nephrol.* **28**, 903–914 (2017).
26. Zajicek, H. K. et al. Glycosphingolipids modulate renal phosphate transport in potassium deficiency. *Kidney Int.* **60**, 694–704 (2001).
27. Inoue, M. et al. Partitioning of NaPi cotransporter in cholesterol-, sphingomyelin-, and glycosphingolipid-enriched membrane domains modulates NaPi protein diffusion, clustering, and activity. *J. Biol. Chem.* **279**, 49160–49171 (2004).
28. Breusegem, S. Y. et al. Differential regulation of the renal sodium-phosphate cotransporters NaPi-IIa, NaPi-IIc, and PiT-2 in dietary potassium deficiency. *Am. J. Physiol. Renal Physiol.* **297**, F350–F361 (2009).
29. Ambuhl, P. M., Zajicek, H. K., Wang, H., Puttaparthi, K. & Levi, M. Regulation of renal phosphate transport by acute and chronic metabolic acidosis in the rat. *Kidney Int.* **53**, 1288–1298 (1998).
30. Nowik, M. et al. Renal phosphaturia during metabolic acidosis revisited: molecular mechanisms for decreased renal phosphate reabsorption. *Pflugers Arch.* **457**, 539–549 (2008).
31. Villa-Bellosta, R. & Sorribas, V. Compensatory regulation of the sodium/phosphate cotransporters NaPi-IIc (SCL34A3) and Pit-2 (SLC20A2) during P_i deprivation and acidosis. *Pflugers Arch.* **459**, 499–508 (2010).
32. Kempson, S. A. et al. Parathyroid hormone action on phosphate transporter mRNA and protein in rat renal proximal tubules. *Am. J. Physiol.* **268**, F784–F791 (1995).
33. Deliot, N. et al. Parathyroid hormone treatment induces dissociation of type IIa Na^+-P(i) cotransporter-Na^+/H^+ exchanger regulatory factor-1 complexes. *Am. J. Physiol. Cell Physiol.* **289**, C159–C167 (2005).
34. Picard, N. et al. Acute parathyroid hormone differentially regulates renal brush border membrane phosphate cotransporters. *Pflugers Arch.* **460**, 677–687 (2010).
35. Segawa, H. et al. Parathyroid hormone-dependent endocytosis of renal type IIc Na-Pi cotransporter. *Am. J. Physiol. Renal Physiol.* **292**, F395–F403 (2007).
36. Lederer, E. D., Khundmiri, S. J. & Weinman, E. J. Role of NHERF-1 in regulation of the activity of Na-K ATPase and sodium-phosphate co-transport in epithelial cells. *J. Am. Soc. Nephrol.* **14**, 1711–1719 (2003).
37. Karim, Z. et al. *NHERF1* mutations and responsiveness of renal parathyroid hormone. *N. Engl. J. Med.* **359**, 1128–1135 (2008).
38. Capuano, P. et al. Defective coupling of apical PTH receptors to phospholipase C prevents internalization of the Na^+-phosphate cotransporter NaPi-IIa in Nherf1-deficient mice. *Am. J. Physiol. Cell Physiol.* **292**, C927–C934 (2007).
39. Mahon, M. J., Donowitz, M., Yun, C. C. & Segre, G. V. Na^+/H^+ exchanger regulatory factor 2 directs parathyroid hormone 1 receptor signalling. *Nature* **417**, 858–861 (2002).

40. Mahon, M. J. & Segre, G. V. Stimulation by parathyroid hormone of a NHERF-1-assembled complex consisting of the parathyroid hormone I receptor, phospholipase Cbeta, and actin increases intracellular calcium in opossum kidney cells. *J. Biol. Chem.* **279**, 23550–23558 (2004).
41. Traebert, M., Volkl, H., Biber, J., Murer, H. & Kaissling, B. Luminal and contraluminal action of 1–34 and 3–34 PTH peptides on renal type IIa Na-P(i) cotransporter. *Am. J. Physiol. Renal Physiol.* **278**, F792–F798 (2000).
42. Lederer, E. D., Sohi, S. S. & McLeish, K. R. Parathyroid hormone stimulates extracellular signal-regulated kinase (ERK) activity through two independent signal transduction pathways: role of ERK in sodium-phosphate cotransport. *J. Am. Soc. Nephrol.* **11**, 222–231 (2000).
43. Bacic, D. et al. Involvement of the MAPK-kinase pathway in the PTH-mediated regulation of the proximal tubule type IIa Na^+/Pi cotransporter in mouse kidney. *Pflugers Arch.* **446**, 52–60 (2003).
44. Keusch, I. et al. Parathyroid hormone and dietary phosphate provoke a lysosomal routing of the proximal tubular Na/Pi-cotransporter type II. *Kidney Int.* **54**, 1224–1232 (1998).
45. Pfister, M. F. et al. Parathyroid hormone leads to the lysosomal degradation of the renal type II Na/Pi cotransporter. *Proc. Natl Acad. Sci. USA* **95**, 1909–1914 (1998).
46. Lotscher, M. et al. Rapid downregulation of rat renal Na/P(i) cotransporter in response to parathyroid hormone involves microtubule rearrangement. *J. Clin. Invest.* **104**, 483–494 (1999).
47. Blaine, J. et al. PTH-induced internalization of apical membrane NaPi2a: role of actin and myosin VI. *Am. J. Physiol. Cell Physiol.* **297**, C1339–C1346 (2009).
48. Lanzano, L. et al. Differential modulation of the molecular dynamics of the type IIa and IIc sodium phosphate cotransporters by parathyroid hormone. *Am. J. Physiol. Cell Physiol.* **301**, C850–C861 (2011).
49. Kurnik, B. R. & Hruska, K. A. Mechanism of stimulation of renal phosphate transport by 1,25-dihydroxycholecalciferol. *Biochim. Biophys. Acta* **817**, 42–50 (1985).
50. Beck, L. et al. Targeted inactivation of *Npt2* in mice leads to severe renal phosphate wasting, hypercalciuria, and skeletal abnormalities. *Proc. Natl Acad. Sci. USA* **95**, 5372–5377 (1998).
51. Capuano, P. et al. Intestinal and renal adaptation to a low-Pi diet of type II NaPi cotransporters in vitamin D receptor- and 1alphaOHase-deficient mice. *Am. J. Physiol. Cell Physiol.* **288**, C429–C434 (2005).
52. Kaneko, I. et al. Hypophosphatemia in vitamin D receptor null mice: effect of rescue diet on the developmental changes in renal Na^+ -dependent phosphate cotransporters. *Pflugers Arch.* **461**, 77–90 (2011).
53. Loffing, J. et al. Renal Na/H exchanger NHE-3 and Na-PO4 cotransporter NaPi-2 protein expression in glucocorticoid excess and deficient states. *J. Am. Soc. Nephrol.* **9**, 1560–1567 (1998).
54. Arar, M., Levi, M. & Baum, M. Maturational effects of glucocorticoids on neonatal brush-border membrane phosphate transport. *Pediatr. Res.* **35**, 474–478 (1994).
55. Frick, A. & Durasin, I. Proximal tubular reabsorption of inorganic phosphate in adrenalectomized rats. *Pflugers Arch.* **385**, 189–192 (1980).
56. Levi, M. et al. Dexamethasone modulates rat renal brush border membrane phosphate transporter mRNA and protein abundance and glycosphingolipid composition. *J. Clin. Invest.* **96**, 207–216 (1995).
57. Arima, K. et al. Glucocorticoid regulation and glycosylation of mouse intestinal type IIb Na-P(i) cotransporter during ontogeny. *Am. J. Physiol. Gastrointest. Liver Physiol.* **283**, G426–G434 (2002).
58. Stock, J. L., Coderre, J. A. & Mallette, L. E. Effects of a short course of estrogen on mineral metabolism in postmenopausal women. *J. Clin. Endocrinol. Metab.* **61**, 595–600 (1985).

59. Faroqui, S., Levi, M., Soleimani, M. & Amlal, H. Estrogen downregulates the proximal tubule type IIa sodium phosphate cotransporter causing phosphate wasting and hypophosphatemia. *Kidney Int.* **73**, 1141–1150 (2008).
60. Xu, H. et al. Regulation of intestinal NaPi-IIb cotransporter gene expression by estrogen. *Am. J. Physiol. Gastrointest. Liver Physiol.* **285**, G1317–G1324 (2003).
61. Burris, D. et al. Estrogen directly and specifically downregulates NaPi-IIa through the activation of both estrogen receptor isoforums (ERalpha and ERbeta) in rat kidney proximal tubule. *Am. J. Physiol. Renal Physiol.* **308**, F522–F534 (2015).
62. Carrillo-Lopez, N. et al. Indirect regulation of PTH by estrogens may require FGF23. *J. Am. Soc. Nephrol.* **20**, 2009–2017 (2009).
63. Alcalde, A. I. et al. Role of thyroid hormone in regulation of renal phosphate transport in young and aged rats. *Endocrinology* **140**, 1544–1551 (1999).
64. Sorribas, V., Markovich, D., Verri, T., Biber, J. & Murer, H. Thyroid hormone stimulation of Na/Pi-cotransport in opossum kidney cells. *Pflugers Arch.* **431**, 266–271 (1995).
65. Euzet, S., Lelievre-Pegorier, M. & Merlet-Benichou, C. Maturation of rat renal phosphate transport: effect of triiodothyronine. *J. Physiol.* **488**, 449–457 (1995).
66. Hu, M. C., Shiizaki, K., Kuro-o, M. & Moe, O. W. Fibroblast growth factor 23 and Klotho: physiology and pathophysiology of an endocrine network of mineral metabolism. *Annu. Rev. Physiol.* **75**, 503–533 (2013).
67. Perwad, F. et al. Dietary and serum phosphorus regulate fibroblast growth factor 23 expression and 1,25-dihydroxyvitamin D metabolism in mice. *Endocrinology* **146**, 5358–5364 (2005).
68. Lavi-Moshayoff, V., Wasserman, G., Meir, T., Silver, J. & Naveh-Many, T. PTH increases FGF23 gene expression and mediates the high-FGF23 levels of experimental kidney failure: a bone parathyroid feedback loop. *Am. J. Physiol. Renal Physiol.* **299**, F882–F889 (2010).
69. Kolek, O. I. et al. 1alpha, 25-Dihydroxyvitamin D3 upregulates FGF23 gene expression in bone: the final link in a renal-gastrointestinal-skeletal axis that controls phosphate transport. *Am. J. Physiol. Gastrointest. Liver Physiol.* **289**, G1036–G1042 (2005).
70. Rodriguez-Ortiz, M. E. et al. Calcium deficiency reduces circulating levels of FGF23. *J. Am. Soc. Nephrol.* **23**, 1190–1197 (2012).
71. Wolf, M. & White, K. E. Coupling fibroblast growth factor 23 production and cleavage: iron deficiency, rickets, and kidney disease. *Curr. Opin. Nephrol. Hypertension* **23**, 411–419 (2014).
72. Daryadel, A. et al. Erythropoietin stimulates fibroblast growth factor 23 (FGF23) in mice and men. *Pflugers Arch.* **470**, 1569–1582 (2018).
73. Bar, L. et al. Insulin suppresses the production of fibroblast growth factor 23 (FGF23). *Proc. Natl Acad. Sci. USA* **115**, 5804–5809 (2018).
74. Glosse, P. et al. AMP-activated kinase is a regulator of fibroblast growth factor 23 production. *Kidney Int.* **94**, 491–501 (2018).
75. Ito, N. et al. Regulation of FGF23 expression in IDG-SW3 osteocytes and human bone by pro-inflammatory stimuli. *Mol. Cell. Endocrinol.* **399**, 208–218 (2015).
76. Urakawa, I. et al. Klotho converts canonical FGF receptor into a specific receptor for FGF23. *Nature* **444**, 770–774 (2006).
77. Saito, H. et al. Human fibroblast growth factor-23 mutants suppress Na^+-dependent phosphate co-transport activity and 1alpha, 25-dihydroxyvitamin D3 production. *J. Biol. Chem.* **278**, 2206–2211 (2003).
78. Weinman, E. J., Steplock, D., Shenolikar, S. & Biswas, R. Fibroblast growth factor-23-mediated inhibition of renal phosphate transport in mice requires sodium-hydrogen exchanger regulatory factor-1 (NHERF-1) and synergizes with parathyroid hormone. *J. Biol. Chem.* **286**, 37216–37221 (2011).
79. Ben-Dov, I. Z. et al. The parathyroid is a target organ for FGF23 in rats. *J. Clin. Invest.* **117**, 4003–4008 (2007).

80. Scanni, R., vonRotz, M., Jehle, S., Hulter, H. N. & Krapf, R. The human response to acute enteral and parenteral phosphate loads. *J. Am. Soc. Nephrol.* **25**, 2730–2739 (2014).
81. Christov, M. et al. Plasma FGF23 levels increase rapidly after acute kidney injury. *Kidney Int.* **84**, 776–785 (2013).
82. White, K. E. et al. Autosomal dominant hypophosphataemic rickets is associated with mutations in FGF23. *Nat. Genet.* **26**, 345–348 (2000).
83. Shimada, T. et al. Cloning and characterization of FGF23 as a causative factor of tumor-induced osteomalacia. *Proc. Natl Acad. Sci. USA* **98**, 6500–6505 (2001).
84. Benet-Pages, A., Orlik, P., Strom, T. M. & Lorenz-Depiereux, B. An FGF23 missense mutation causes familial tumoral calcinosis with hyperphosphatemia. *Hum. Mol. Genet.* **14**, 385–390 (2005).
85. Ichikawa, S. et al. A homozygous missense mutation in human KLOTHO causes severe tumoral calcinosis. *J. Clin. Invest.* **117**, 2684–2691 (2007).
86. Shimada, T. et al. Targeted ablation of Fgf23 demonstrates an essential physiological role of FGF23 in phosphate and vitamin D metabolism. *J. Clin. Invest.* **113**, 561–568 (2004).
87. Gattineni, J. et al. FGF23 decreases renal NaPi-2a and NaPi-2c expression and induces hypophosphatemia in vivo predominantly via FGF receptor 1. *Am. J. Physiol. Renal Physiol.* **297**, F282–F291 (2009).
88. Gattineni, J. et al. Regulation of renal phosphate transport by FGF23 is mediated by FGFR1 and FGFR4. *Am. J. Physiol. Renal Physiol.* **306**, F351–F358 (2014).
89. Komaba, H. et al. Depressed expression of Klotho and FGF receptor 1 in hyperplastic parathyroid glands from uremic patients. *Kidney Int.* **77**, 232–238 (2010).
90. White, K. E. et al. Mutations that cause osteoglophonic dysplasia define novel roles for FGFR1 in bone elongation. *Am. J. Hum. Genet.* **76**, 361–367 (2005).
91. Hu, M. C. et al. Klotho: a novel phosphaturic substance acting as an autocrine enzyme in the renal proximal tubule. *FASEB J.* **24**, 3438–3450 (2010).
92. Chen, G. Z. et al. alpha-Klotho is a non-enzymatic molecular scaffold for FGF23 hormone signalling. *Nature* **553**, 461–466 (2018).
93. Brownstein, C. A. et al. A translocation causing increased alpha-Klotho level results in hypophosphatemic rickets and hyperparathyroidism. *Proc. Natl Acad. Sci. USA* **105**, 3455–3460 (2008).
94. Kato, K. et al. Polypeptide GalNAc-transferase T3 and familial tumoral calcinosis. Secretion of fibroblast growth factor 23 requires O-glycosylation. *J. Biol. Chem.* **281**, 18370–18377 (2006).
95. Topaz, O. et al. Mutations in *GALNT3*, encoding a protein involved in O-linked glycosylation, cause familial tumoral calcinosis. *Nat. Genet.* **36**, 579–581 (2004).
96. Ichikawa, S. et al. Ablation of the Galnt3 gene leads to low-circulating intact fibroblast growth factor 23 (Fgf23) concentrations and hyperphosphatemia despite increased Fgf23 expression. *Endocrinology* **150**, 2543–2550 (2009).
97. Ichikawa, S. et al. Genetic rescue of glycosylation-deficient Fgf23 in the *Galnt3* knockout mouse. *Endocrinology* **155**, 3891–3898 (2014).
98. Ito, N., Findlay, D. M., Anderson, P. H., Bonewald, L. F. & Atkins, G. J. Extracellular phosphate modulates the effect of 1alpha, 25-dihydroxy vitamin D3 (1,25D) on osteocyte like cells. *J. Steroid Biochem. Mol. Biol.* **136**, 183–186 (2013).
99. Fan, Y. et al. Parathyroid hormone 1 receptor is essential to induce FGF23 production and maintain systemic mineral ion homeostasis. *FASEB J.* **30**, 428–440 (2016).
100. Chefetz, I. et al. GALNT3, a gene associated with hyperphosphatemic familial tumoral calcinosis, is transcriptionally regulated by extracellular phosphate and modulates matrix metalloproteinase activity. *Biochim. Biophys. Acta* **1792**, **61–67**, (2009).
101. Francis, F. et al. A gene (*PEX*) with homologies to endopeptidases is mutated in patients with X-linked hypophosphatemic rickets. *Nat. Genet.* **11**, 130–136 (1995).

102. Rowe, P. S. Regulation of bone-renal mineral and energy metabolism: the PHEX, FGF23, DMP1, MEPE ASARM pathway. *Crit. Rev. Eukaryot. Gene Expr.* **22**, 61–86 (2012).
103. Tenenhouse, H. S., Martel, J., Gauthier, C., Segawa, H. & Miyamoto, K. Differential effects of Npt2a gene ablation and X-linked Hyp mutation on renal expression of Npt2c. *Am. J. Physiol. Renal Physiol.* **285**, F1271–F1278 (2003).
104. Yuan, B. et al. Hexa-D-arginine treatment increases 7B2*PC2 activity in hyp-mouse osteoblasts and rescues the HYP phenotype. *J. Bone Miner. Res.* **28**, 56–72 (2013).
105. Rowe, P. S. et al. MEPE, a new gene expressed in bone marrow and tumors causing osteomalacia. *Genomics* **67**, 54–68 (2000).
106. Bresler, D., Bruder, J., Mohnike, K., Fraser, W. D. & Rowe, P. S. Serum MEPE-ASARM-peptides are elevated in X-linked rickets (HYP): implications for phosphaturia and rickets. *J. Endocrinol.* **183**, R1–R9 (2004).
107. Rowe, P. S. et al. MEPE has the properties of an osteoblastic phosphatonin and minhibin. *Bone* **34**, 303–319 (2004).
108. Marks, J., Churchill, L. J., Debnam, E. S. & Unwin, R. J. Matrix extracellular phosphoglycoprotein inhibits phosphate transport. *J. Am. Soc. Nephrol.* **19**, 2313–2320 (2008).
109. Aniteli, T. M. et al. Effect of variations in dietary P_i intake on intestinal P_i transporters (NaPi-IIb, PiT-1, and PiT-2) and phosphate-regulating factors (PTH, FGF-23, and MEPE). *Pflugers Arch.* **470**, 623–632 (2018).
110. Argiro, L., Desbarats, M., Glorieux, F. H. & Ecarot, B. Mepe, the gene encoding a tumor-secreted protein in oncogenic hypophosphatemic osteomalacia, is expressed in bone. *Genomics* **74**, 342–351 (2001).
111. Toyosawa, S. et al. Expression of dentin matrix protein 1 in tumors causing oncogenic osteomalacia. *Mod. Pathol.* **17**, 573–578 (2004).
112. Lorenz-Depiereux, B. et al. *DMP1* mutations in autosomal recessive hypophosphatemia implicate a bone matrix protein in the regulation of phosphate homeostasis. *Nat. Genet.* **38**, 1248–1250 (2006).
113. Feng, J. Q. et al. Loss of DMP1 causes rickets and osteomalacia and identifies a role for osteocytes in mineral metabolism. *Nat. Genet.* **38**, 1310–1315 (2006).
114. Martin, A. et al. Bone proteins PHEX and DMP1 regulate fibroblastic growth factor Fgf23 expression in osteocytes through a common pathway involving FGF receptor (FGFR) signaling. *FASEB J.* **25**, 2551–2562 (2011).
115. Wang, L. et al. PTH and vitamin D repress DMP1 in cementoblasts. *J. Dent. Res.* **94**, 1408–1416 (2015).
116. Berndt, T. et al. Secreted frizzled-related protein 4 is a potent tumor-derived phosphaturic agent. *J. Clin. Invest.* **112**, 785–794 (2003).
117. Hsieh, J. C. et al. A new secreted protein that binds to Wnt proteins and inhibits their activities. *Nature* **398**, 431–436 (1999).
118. Cho, H. Y. et al. Transgenic mice overexpressing secreted frizzled-related proteins (sFRP)4 under the control of serum amyloid P promoter exhibit low bone mass but did not result in disturbed phosphate homeostasis. *Bone* **47**, 263–271 (2010).
119. Zinkle, A. & Mohammadi, M. Structural biology of the FGF7 subfamily. *Front. Genet.* **10**, 102 (2019).
120. Carpenter, T. O. et al. Fibroblast growth factor 7: an inhibitor of phosphate transport derived from oncogenic osteomalacia-causing tumors. *J. Clin. Endocrinol. Metab.* **90**, 1012–1020 (2005).
121. Hernando, N. NaPi-IIa interacting partners and their (un)known functional roles. *Pflugers Arch.* **471**, 67–82 (2018).
122. Biber, J., Gisler, S. M., Hernando, N., Wagner, C. A. & Murer, H. PDZ interactions and proximal tubular phosphate reabsorption. *Am. J. Physiol. Renal Physiol.* **287**, F871–F875 (2004).

123. Weinman, E. J., Steplock, D., Wang, Y. & Shenolikar, S. Characterization of a protein cofactor that mediates protein kinase A regulation of the renal brush border membrane Na^+-H^+ exchanger. *J. Clin. Invest.* **95**, 2143–2149 (1995).
124. Donowitz, M. et al. NHERF family and NHE3 regulation. *J. Physiol.* **567**, 3–11 (2005).
125. Hernando, N. et al. NaPi-IIa and interacting partners. *J. Physiol.* **567**, 21–26 (2005).
126. Thelin, W. R., Hodson, C. A. & Milgram, S. L. Beyond the brush border: NHERF4 blazes new NHERF turf. *J. Physiol.* **567**, 13–19 (2005).
127. Weinman, E. J., Cunningham, R., Wade, J. B. & Shenolikar, S. The role of NHERF-1 in the regulation of renal proximal tubule sodium-hydrogen exchanger 3 and sodium-dependent phosphate cotransporter 2a. *J. Physiol.* **567**, 27–32 (2005).
128. Yun, C. H. et al. cAMP-mediated inhibition of the epithelial brush border Na^+/H^+ exchanger, NHE3, requires an associated regulatory protein. *Proc. Natl Acad. Sci. USA* **94**, 3010–3015 (1997).
129. Dobrinskikh, E., Giral, H., Caldas, Y. A., Levi, M. & Doctor, R. B. Shank2 redistributes with NaPilla during regulated endocytosis. *Am. J. Physiol. Cell Physiol.* **299**, C1324–C1334 (2010).
130. Lanaspa, M. A. et al. Inorganic phosphate modulates the expression of the NaPi-2a transporter in the *trans*-Golgi network and the interaction with PIST in the proximal tubule. *Biomed. Res. Int.* **2013**, 513932 (2013).
131. Villa-Bellosta, R. et al. Interactions of the growth-related, type IIc renal sodium/phosphate cotransporter with PDZ proteins. *Kidney Int.* **73**, 456–464 (2008).
132. Hernando, N. et al. PDZ-domain interactions and apical expression of type IIa Na/P(i) cotransporters. *Proc. Natl Acad. Sci. USA* **99**, 11957–11962 (2002).
133. Weinman, E. J. et al. NHERF-1 is required for renal adaptation to a low-phosphate diet. *Am. J. Physiol. Renal Physiol.* **285**, F1225–F1232 (2003).
134. Wang, B. et al. Ezrin-anchored protein kinase A coordinates phosphorylation-dependent disassembly of a NHERF1 ternary complex to regulate hormone-sensitive phosphate transport. *J. Biol. Chem.* **287**, 24148–24163 (2012).
135. Giral, H. et al. NHE3 regulatory factor 1 (NHERF1) modulates intestinal sodium-dependent phosphate transporter (NaPi-2b) expression in apical microvilli. *J. Biol. Chem.* **287**, 35047–35056 (2012).
136. Gisler, S. M. et al. PDZK1: I. a major scaffolder in brush borders of proximal tubular cells. *Kidney Int.* **64**, 1733–1745 (2003).
137. Hernando, N. et al. NaPi-IIa interacting proteins and regulation of renal reabsorption of phosphate. *Urol. Res.* **38**, 271–276 (2010).
138. Giral, H. et al. Role of PDZK1 protein in apical membrane expression of renal sodium-coupled phosphate transporters. *J. Biol. Chem.* **286**, 15032–15042 (2011).
139. McWilliams, R. R. et al. Shank2E binds NaP(i) cotransporter at the apical membrane of proximal tubule cells. *Am. J. Physiol. Cell Physiol.* **289**, C1042–C1051 (2005).
140. Dobrinskikh, E. et al. Shank2 contributes to the apical retention and intracellular redistribution of NaPiIIa in OK cells. *Am. J. Physiol. Cell Physiol.* **304**, C561–C573 (2013).
141. Gisler, S. M. et al. Monitoring protein-protein interactions between the mammalian integral membrane transporters and PDZ-interacting partners using a modified split-ubiquitin membrane yeast two-hybrid system. *Mol. Cell. Proteomics* **7**, 1362–1377 (2008).
142. Levi, M., Jameson, D. M. & van der Meer, B. W. Role of BBM lipid composition and fluidity in impaired renal P_i transport in aged rat. *Am. J. Physiol.* **256**, F85–F94 (1989).
143. Sorribas, V. et al. Cellular mechanisms of the age-related decrease in renal phosphate reabsorption. *Kidney Int.* **50**, 855–863 (1996).

144. Breusegem, S. Y. et al. Acute and chronic changes in cholesterol modulate Na-Pi cotransport activity in OK cells. *Am. J. Physiol. Renal Physiol.* **289**, F154–F165 (2005).
145. Levi, M., Baird, B. M. & Wilson, P. V. Cholesterol modulates rat renal brush border membrane phosphate transport. *J. Clin. Invest.* **85**, 231–237 (1990).
146. Levi, M., Wilson, P. V., Cooper, O. J. & Gratton, E. Lipid phases in renal brush border membranes revealed by Laurdan fluorescence. *Photochem. Photobiol.* **57**, 420–425 (1993).
147. Parasassi, T., Gratton, E., Zajicek, H., Levi, M. & Yu, W. Detecting membrane lipid microdomains by two-photon fluorescence microscopy. *IEEE Eng. Med. Biol. Mag.* **18**, 92–99 (1999).
148. Dietrich, C. et al. Lipid rafts reconstituted in model membranes. *Biophys. J.* **80**, 1417–1428 (2001).
149. Dietrich, C., Volovyk, Z. N., Levi, M., Thompson, N. L. & Jacobson, K. Partitioning of Thy-1, GM1, and cross-linked phospholipid analogs into lipid rafts reconstituted in supported model membrane monolayers. *Proc. Natl Acad. Sci. USA* **98**, 10642–10647 (2001).
150. Ruan, Q., Cheng, M. A., Levi, M., Gratton, E. & Mantulin, W. W. Spatial-temporal studies of membrane dynamics: scanning fluorescence correlation spectroscopy (SFCS). *Biophys. J.* **87**, 1260–1267 (2004).
151. Kestenbaum, B. et al. Common genetic variants associate with serum phosphorus concentration. *J. Am. Soc. Nephrol.* **21**, 1223–1232 (2010).
152. Monico, C. G. & Milliner, D. S. Genetic determinants of urolithiasis. *Nat. Clin. Pract. Nephrol.* **8**, 151–162 (2012).
153. Oddsson, A. et al. Common and rare variants associated with kidney stones and biochemical traits. *Nat. Commun.* **6**, 7975 (2015).
154. Prie, D. et al. Nephrolithiasis and osteoporosis associated with hypophosphatemia caused by mutations in the type 2a sodium-phosphate cotransporter. *N. Engl. J. Med.* **347**, 983–991 (2002).
155. Rajagopal, A. et al. Exome sequencing identifies a novel homozygous mutation in the phosphate transporter SLC34A1 in hypophosphatemia and nephrocalcinosis. *J. Clin. Endocrinol. Metab.* **99**, E2451–E2456 (2014).
156. Schlingmann, K. P. et al. Autosomal-recessive mutations in SLC34A1 encoding sodium-phosphate cotransporter 2A cause idiopathic infantile hypercalcemia. *J. Am. Soc. Nephrol.* **27**, 604–614 (2016).
157. Braun, D. A. et al. Prevalence of monogenic causes in pediatric patients with nephrolithiasis or nephrocalcinosis. *Clin. J. Am. Soc. Nephrol.* **11**, 664–672 (2016).
158. Halbritter, J. et al. Fourteen monogenic genes account for 15% of nephrolithiasis/nephrocalcinosis. *J. Am. Soc. Nephrol.* **26**, 543–551 (2015).
159. Dinour, D. et al. Loss of function of NaPiIIa causes nephrocalcinosis and possibly kidney insufficiency. *Pediatr. Nephrol.* **31**, 2289–2297 (2016).
160. Magen, D. et al. A loss-of-function mutation in NaPi-IIa and renal Fanconi's syndrome. *N. Engl. J. Med.* **362**, 1102–1109 (2010).
161. Hureaux, M. et al. Prenatal hyperechogenic kidneys in three cases of infantile hypercalcemia associated with SLC34A1 mutations. *Pediatr. Nephrol.* **33**, 1723–1729 (2018).
162. Fearn, A. et al. Clinical, biochemical, and pathophysiological analysis of SLC34A1 mutations. *Physiol. Rep.* **6**, e13715 (2018).
163. Kenny, J. et al. Sotos syndrome, infantile hypercalcemia, and nephrocalcinosis: a contiguous gene syndrome. *Pediatr. Nephrol.* **26**, 1331–1334 (2011).
164. Pronicka, E. et al. Biallelic mutations in *CYP24A1* or *SLC34A1* as a cause of infantile idiopathic hypercalcemia (IIH) with vitamin D hypersensitivity: molecular study of 11 historical IIH cases. *J. Appl. Genet.* **58**, 349–353 (2017).
165. Amar, A. et al. Gene panel sequencing identifies a likely monogenic cause in 7% of 235 Pakistani families with nephrolithiasis. *Hum. Genet.* **138**, 211–219 (2019).

166. Lapointe, J.-Y. et al. *NPT2a* gene variation in calcium nephrolithiasis with renal phosphate leak. *Kidney Int.* **69**, 2261–2267 (2006).
167. Köhler, K., Forster, I. C., Lambert, G., Biber, J. & Murer, H. The functional unit of the renal type IIa Na^+/P_i cotransporter is a monomer. *J. Biol. Chem.* **275**, 26113–26120 (2000).
168. Khan, S. R. & Glenton, P. A. Calcium oxalate crystal deposition in kidneys of hypercalciuric mice with disrupted type IIa sodium-phosphate cotransporter. *Am. J. Physiol. Renal Physiol.* **294**, F1109–F1115 (2008).
169. Chau, H., El-Maadawy, S., McKee, M. D. & Tenenhouse, H. S. Renal calcification in mice homozygous for the disrupted type IIa Na/Pi cotransporter gene Npt2. *J. Bone Miner. Res.* **18**, 644–657 (2003).
170. Tenenhouse, H. S., Gauthier, C., Chau, H. & St-Arnaud, R. 1alpha-Hydroxylase gene ablation and P_i supplementation inhibit renal calcification in mice homozygous for the disrupted Npt2a gene. *Am. J. Physiol. Renal Physiol.* **286**, F675–F681 (2004).
171. Dasgupta, D. et al. Mutations in *SLC34A3/NPT2c* are associated with kidney stones and nephrocalcinosis. *J. Am. Soc. Nephrol.* **25**, 2366–2375 (2014).
172. Lorenz-Depiereux, B. et al. Hereditary hypophosphatemic rickets with hypercalciuria is caused by mutations in the sodium-phosphate cotransporter gene SLC34A3. *Am. J. Hum. Genet.* **78**, 193–201 (2006).
173. Bergwitz, C. et al. *SLC34A3* mutations in patients with hereditary hypophosphatemic rickets with hypercalciuria predict a key role for the sodium-phosphate cotransporter NaP(i)-IIc in maintaining phosphate homeostasis. *Am. J. Hum. Genet.* **78**, 179–192 (2006).
174. Bergwitz, C. & Miyamoto, K. I. Hereditary hypophosphatemic rickets with hypercalciuria: pathophysiology, clinical presentation, diagnosis and therapy. *Pflugers Arch.* **471**, 149–163 (2019).
175. Segawa, H. et al. Type IIc sodium-dependent phosphate transporter regulates calcium metabolism. *J. Am. Soc. Nephrol.* **20**, 104–113 (2009).
176. Myakala, K. et al. Renal-specific and inducible depletion of NaPi-IIc/Slc34a3, the cotransporter mutated in HHRH, does not affect phosphate or calcium homeostasis in mice. *Am. J. Physiol. Renal Physiol.* **306**, F833–F843 (2014).
177. Corut, A. et al. Mutations in *SLC34A2* cause pulmonary alveolar microlithiasis and are possibly associated with testicular microlithiasis. *Am. J. Hum. Genet.* **79**, 650–656 (2006).
178. Ferreira Francisco, F. A., Pereira e Silva, J. L., Hochhegger, B., Zanetti, G. & Marchiori, E. Pulmonary alveolar microlithiasis. State-of-the-art review. *Respir. Med.* **107**, 1–9 (2013).
179. Huqun et al. Mutations in the *SLC34A2* gene are associated with pulmonary alveolar microlithiasis. *Am. J. Respir. Crit. Care Med.* **175**, 263–268 (2007).
180. Traebert, M., Hattenhauer, O., Murer, H., Kaissling, B. & Biber, J. Expression of type II Na-P(i) cotransporter in alveolar type II cells. *Am. J. Physiol.* **277**, L868–L873 (1999).
181. Ma, T. et al. Effect of *SLC34A2* gene mutation on extracellular phosphorus transport in PAM alveolar epithelial cells. *Exp. Ther. Med.* **15**, 310–314 (2018).
182. Hernando, N. et al. Intestinal depletion of NaPi-IIb/Slc34a2 in mice: renal and hormonal adaptation. *J. Bone Miner. Res.* **30**, 1925–1937 (2015).
183. Sabbagh, Y. et al. Intestinal npt2b plays a major role in phosphate absorption and homeostasis. *J. Am. Soc. Nephrol.* **20**, 2348–2358 (2009).
184. Saito, A. et al. Modeling pulmonary alveolar microlithiasis by epithelial deletion of the Npt2b sodium phosphate cotransporter reveals putative biomarkers and strategies for treatment. *Sci. Transl Med.* **7**, 313ra181 (2015).
185. Busch, A. et al. Electrophysiological analysis of Na^+/P_i cotransport mediated by a transporter cloned from rat kidney and expressed in *Xenopus* oocytes. *Proc. Natl Acad. Sci. USA* **91**, 8205–8208 (1994).

186. Forster, I. C., Loo, D. D. & Eskandari, S. Stoichiometry and Na^+ binding cooperativity of rat and flounder renal type II Na^+-P_i cotransporters. *Am. J. Physiol.* **276**, F644–F649 (1999).
187. Bacconi, A., Virkki, L. V., Biber, J., Murer, H. & Forster, I. C. Renouncing electrogenicity is not free of charge: switching on electrogenicity in a Na^+-coupled phosphate cotransporter. *Proc. Natl Acad. Sci. USA* **102**, 12606–12611 (2005).
188. Forster, I. C. The molecular mechanism of SLC34 proteins: insights from two decades of transport assays and structure-function studies. *Pflugers Arch.* **471**, 15–42 (2018).
189. Patti, M., Ghezzi, C. & Forster, I. C. Conferring electrogenicity to the electroneutral phosphate cotransporter NaPi-IIc (SLC34A3) reveals an internal cation release step. *Pflugers Arch.* **465**, 1261–1279 (2013).
190. Bezanilla, F. Gating currents. *J. Gen. Physiol.* **150**, 911–932 (2018).
191. Ghezzi, C., Murer, H. & Forster, I. C. Substrate interactions of the electroneutral Na^+-coupled inorganic phosphate cotransporter (NaPi-IIc). *J. Physiol.* **587**, 4293–4307 (2009).
192. Fenollar-Ferrer, C. et al. Identification of the first sodium binding site of the phosphate cotransporter NaPi-IIa (SLC34A1). *Biophys. J.* **108**, 2465–2480 (2015).
193. Forster, I. C., Biber, J. & Murer, H. Proton-sensitive transitions of renal type II Na(+)-coupled phosphate cotransporter kinetics. *Biophys. J.* **79**, 215–230 (2000).
194. Forster, I. C., Virkki, L. V., Bossi, E., Murer, H. & Biber, J. Electrogenic kinetics of a mammalian intestinal Na^+/P_i-cotransporter. *J. Membr. Biol.* **212**, 177–190 (2006).
195. Hartmann, C. M. et al. Transport characteristics of a murine renal Na/Pi-cotransporter. *Pflugers Archiv.* **430**, 830–836 (1995).
196. Andrini, O., Meinild, A. K., Ghezzi, C., Murer, H. & Forster, I. C. Lithium interactions with Na^+-coupled inorganic phosphate cotransporters: insights into the mechanism of sequential cation binding. *Am. J. Physiol. Cell Physiol.* **302**, C539–C554 (2012).
197. Virkki, L. V., Murer, H. & Forster, I. C. Voltage clamp fluorometric measurements on a type II Na^+-coupled P_i cotransporter: shedding light on substrate binding order. *J. Gen. Physiol.* **127**, 539–555 (2006).
198. Forster, I. C., Hernando, N., Biber, J. & Murer, H. Proximal tubular handling of phosphate: a molecular perspective. *Kidney Int.* **70**, 1548–1559 (2006).
199. Vergara-Jaque, A., Fenollar-Ferrer, C., Mulligan, C., Mindell, J. A. & Forrest, L. R. Family resemblances: a common fold for some dimeric ion-coupled secondary transporters. *J. Gen. Physiol.* **146**, 423–434 (2015).
200. Kohler, K., Forster, I. C., Lambert, G., Biber, J. & Murer, H. The functional unit of the renal type IIa Na^+/Pi cotransporter is a monomer. *J. Biol. Chem.* **275**, 26113–26120 (2000).
201. Fenollar-Ferrer, C. et al. Structural fold and binding sites of the human Na^+-phosphate cotransporter NaPi-II. *Biophys. J.* **106**, 1268–1279 (2014).
202. Forster, I. C., Kohler, K., Biber, J. & Murer, H. Forging the link between structure and function of electrogenic cotransporters: the renal type IIa Na^+/P_i cotransporter as a case study. *Prog. Biophys. Mol. Biol.* **80**, 69–108 (2002).
203. Mitchell, P. A general theory of membrane transport from studies of bacteria. *Nature* **180**, 134–136 (1957).
204. Mulligan, C. et al. The bacterial dicarboxylate transporter VcINDY uses a two-domain elevator-type mechanism. *Nat. Struct. Mol. Biol.* **23**, 256–263 (2016).
205. Patti, M., Fenollar-Ferrer, C., Werner, A., Forrest, L. R. & Forster, I. C. Cation interactions and membrane potential induce conformational changes in NaPi-IIb. *Biophys. J.* **111**, 973–988 (2016).
206. Sorribas, V., Guillen, N. & Sosa, C. Substrates and inhibitors of phosphate transporters: from experimental tools to pathophysiological relevance. *Pflugers Arch.* **471**, 53–65 (2019).

207. Szczepanska-Konkel, M., Yusufi, A. N., VanScoy, M., Webster, S. K. & Dousa, T. P. Phosphonocarboxylic acids as specific inhibitors of Na^+-dependent transport of phosphate across renal brush border membrane. *J. Biol. Chem.* **261**, 6375–6383 (1986).
208. Villa-Bellosta, R. & Sorribas, V. Role of rat sodium/phosphate cotransporters in the cell membrane transport of arsenate. *Toxicol. Appl. Pharmacol.* **232**, 125–134 (2008).
209. Villa-Bellosta, R., Bogaert, Y. E., Levi, M. & Sorribas, V. Characterization of phosphate transport in rat vascular smooth muscle cells: implications for vascular calcification. *Arterioscler. Thromb. Vasc. Biol.* **27**, 1030–1036 (2007).
210. Forster, I., Hernando, N., Biber, J. & Murer, H. The voltage dependence of a cloned mammalian renal type II Na^+/Pi cotransporter (NaPi-2). *J. Gen. Physiol.* **112**, 1–18 (1998).
211. VanScoy, M. et al. Mechanism of phosphaturia elicited by administration of phosphonoformate in vivo. *Am. J. Physiol.* **255**, F984–F994 (1988).
212. Loghman-Adham, M. & Motock, G. T. Use of phosphonoformic acid to induce phosphaturia in chronic renal failure in rats. *Ren. Fail.* **18**, 855–866 (1996).
213. Becker, B. N. & Schulman, G. Nephrotoxicity of antiviral therapies. *Curr. Opin. Nephrol. Hypertens.* **5**, 375–379 (1996).
214. Villa-Bellosta, R. & Sorribas, V. Different effects of arsenate and phosphonoformate on P(i) transport adaptation in opossum kidney cells. *Am. J. Physiol. Cell Physiol.* **297**, C516–C525 (2009).
215. Kempson, S. A., Turner, S. T., Yusufi, A. N. & Dousa, T. P. Actions of NAD^+ on renal brush border transport of phosphate in vivo and in vitro. *Am. J. Physiol.* **249**, F948–F955 (1985).
216. Katai, K. et al. Nicotinamide inhibits sodium-dependent phosphate cotransport activity in rat small intestine. *Nephrol. Dial. Transplant.* **14**, 1195–1201 (1999).
217. Kempson, S. A., Colon-Otero, G., Ou, S. Y., Turner, S. T. & Dousa, T. P. Possible role of nicotinamide adenine dinucleotide as an intracellular regulator of renal transport of phosphate in the rat. *J. Clin. Invest.* **67**, 1347–1360 (1981).
218. Nomura, K. et al. Hepatectomy-related hypophosphatemia: a novel phosphaturic factor in the liver-kidney axis. *J. Am. Soc. Nephrol.* **25**, 761–772 (2014).
219. Miyagawa, A. et al. The sodium phosphate cotransporter family and nicotinamide phosphoribosyltransferase contribute to the daily oscillation of plasma inorganic phosphate concentration. *Kidney Int.* **93**, 1073–1085 (2018).
220. Labonte, E. D. et al. Gastrointestinal inhibition of sodium-hydrogen exchanger 3 reduces phosphorus absorption and protects against vascular calcification in CKD. *J. Am. Soc. Nephrol.* **26**, 1138–1149 (2015).
221. King, A. J. et al. Inhibition of sodium/hydrogen exchanger 3 in the gastrointestinal tract by tenapanor reduces paracellular phosphate permeability. *Sci. Transl Med.* **10**, eaam6474 (2018).
222. Filipski, K. J. et al. Discovery of orally bioavailable selective inhibitors of the sodium-phosphate cotransporter NaPi2a (SLC34A1). *ACS Med. Chem. Lett.* **9**, 440–445 (2018).
223. Hortells, L. et al. Identifying early pathogenic events during vascular calcification in uremic rats. *Kidney Int.* **92**, 1384–1394 (2017).
224. Matsuo, A. et al. Inhibitory effect of JTP-59557, a new triazole derivative, on intestinal phosphate transport in vitro and in vivo. *Eur. J. Pharmacol.* **517**, 111–119 (2005).
225. Larsson, T. E. et al. NPT-IIb inhibition does not improve hyperphosphatemia in CKD. *Kidney Int. Rep.* **3**, 73–80 (2018).
226. Andrini, O., Ghezzi, C., Murer, H. & Forster, I. C. The leak mode of type II Na(+)-P(i) cotransporters. *Channels* **2**, 346–357 (2008).

Acknowledgements

The authors thank X. Wang and K. Myakala, Georgetown University, for help formatting the references.

Ethics declarations

Competing interests

The authors declare no competing interests.

Glossary

Micropuncture

> A technique that uses one or more microelectrodes inserted into the glomerulus, renal vessels or specific nephron segments of the kidney in situ to measure glomerular filtration, blood flow or tubular transport processes.

Brush-border membrane vesicles

> (BBMVs). Sealed vesicles derived from the brush-border membrane of epithelial cells that are frequently used to study the apical transport of solutes across the apical membrane in vitro. They are obtained upon homogenization of the tissue and precipitation of basolateral membranes with $MgCl_2$.

Lysosomes

> Intracellular acidic organelles that contain enzymes that are able to hydrolyse protein, sugars, lipids, RNA and DNA. These enzymes have an acidic optimal pH. Among other substrates, they digest endocytosed material.

Microtubule

> A component of the cytoskeleton consisting of polymers of tubulin. They are involved in several cellular processes, including intracellular transport of cargo vesicles to and from the plasma membrane using kinesin or dynein as motor proteins.

Subapical endocytic apparatus

> (SEA). A subapical domain of epithelial cells consisting of clathrin-coated pits, endocytic vesicles and membrane-limited tubules called dense apical tubules. These tubules have been proposed to contribute to the sorting and recycling of endocytic cargo and receptors.

Total internal reflection fluorescence (TIRF) microscopy

A technique whereby total internal reflection of the excitation light limits fluorescence detection to approximately 100 nm above the glass or the apical membrane.

Modulation tracking

An orbital tracking method for single particle tracking based on active feedback, which moves microvilli to maintain them within the centre of a scanned pattern.

Raster image correlation spectroscopy

(RICS). A non-invasive technique that detects and quantifies events in a live cell, including the concentration of molecules and diffusion coefficients of molecules.

Number and brightness (N&B) analysis

A technique based on moment analysis for measuring the average number of molecules and brightness in each pixel in fluorescence microscopy images.

Autosomal dominant hypophosphataemic rickets

(ADHR). A rare hereditary disease that has an autosomal dominant mode of inheritance and variable age of onset and is caused by mutations that increase the half-life of *FGF23*. It is characterized by renal phosphate wasting, hypophosphataemia and inappropriately normal levels of 1,25-dihydroxy-vitamin D_3, with patients suffering from bone pain and rickets.

Tumour-induced osteomalacia

Also known as oncogenic hypophosphataemic osteomalacia. A rare syndrome caused by small tumours that secrete fibroblast growth factor 23 (FGF23), matrix extracellular phosphoglycoprotein (MEPE) and secreted frizzled-related protein 4 (sFRP4). It is characterized by hypophosphataemia due to urinary loss of inorganic phosphate, bone pain and fractures and muscle weakness.

Familial tumoural calcinosis

(FTC). Also known as hyperphosphataemic FTC. A rare autosomal hereditary disorder characterized by hyperphosphataemia due to inactivating mutations in the *FGF23*, *GALNT3* or *KL* genes and by secondary to reduced urinary excretion of inorganic phosphate, normal or elevated 1,25-dihydroxy-vitamin D_3 and ectopic calcification.

Hypomorphic

A hypomorphic mutation is one that results in reduced activity of the encoded protein.

Osteoglophonic dysplasia

A rare autosomal dominant disease caused by mutations in the fibroblast growth factor receptor 1 (FGFR1). Patients exhibit hypophosphataemia due to hyperphosphaturia and abnormal bone growth that results in severe craniofacial abnormalities, short and bowed legs and arms and dwarfism.

X-Linked hypophosphataemic rickets

(XLH). An X-linked hypophosphataemic disease secondary to renal loss of inorganic phosphate caused by mutations in phosphate-regulating neutral endopeptidase (PHEX). Patients suffer from rickets, bone and/or dental deformities and have short stature.

Autosomal recessive hypophosphataemic rickets

(ARHR1). Similar biochemical and phenotypical features as autosomal dominant hypophosphataemic rickets, but with a recessive mode of inheritance. It is caused by mutations in *DMP1* (among others).

Fluorescence lifetime imaging microscopy and Förster resonance energy transfer

(FLIM-FRET). A microscopy system that enables determination of protein–protein interactions within 10 nm or less in live cells on the basis of changing lifetimes of the fluorophores.

Sphingomyelin

A phospholipid enriched in saturated fatty acids that is part of the lipid rafts.

BBM fluidity

A measure of the lipid dynamics of the apical brush-border membrane.

Fluorescence anisotropy of diphenylhexatriene

Measurement of the membrane fluidity. A higher value indicates a less fluid membrane.

Lipid microdomains

Also known as lipid rafts. Regions of the membrane that may be smaller than the 200 nm size of the diffraction barrier and that may be dynamic in nature.

Laurdan fluorescence spectroscopy

Laurdan is a fluorescent molecule that is highly sensitive to water penetration and cholesterol within the membrane lipid bilayer.

Glucosylceramide

A membrane glycosphingolipid that is associated with lipid raft formation.

Multiphoton excitation (MPE) fluorescence microscopy

A nonlinear microscopy system in which the exciting light is provided by a two-photon near-infrared laser.

Scanning fluorescence correlation spectroscopy

(SFCS). A technique that performs multiple fluorescence correlation spectroscopy measurements simultaneously by rapidly directing the excitation laser beam in a uniform (circular) scan across the bilayer of the cell membrane in a repetitive fashion. SFCS provides a quantitative and highly sensitive method to study protein diffusion and protein–membrane interactions.

Sotos syndrome

An inborn syndrome characterized by accelerated body length growth, microcephalus and delayed cognitive and motor development. It is caused by deletions on chromosome 5q35 encompassing the *NSD1* gene neighbouring the *SLC34A1* gene locus.

Compound heterozygosity

Two different recessive mutations of a particular gene.

Minor allele frequency

The frequency at which the second most common allele occurs in a given population.

Hereditary hypophosphataemic rickets with hypercalciuria

(HHRH). An autosomal recessive form caused by mutations in *SLC34A3* and characterized by reduced renal phosphate reabsorption, hypophosphataemia, and rickets. It can be distinguished from other forms of hypophosphataemia by increased serum levels of 1,25-dihydroxy-vitamin D_3 resulting in hypercalciuria.

Pulmonary alveolar microlithiasis

(PAM). A chronic, slowly fibrosing lung disease caused and characterized by calcium-phosphate microcrystal depositions in the alveolar space.

Cor pulmonale

Right ventricular enlargement secondary to a lung disorder that causes pulmonary arterial hypertension.

Testicular microlithiasis

An asymptomatic deposition of small crystals in testes. It may be associated with the risk of infertility or testicular cancer, but a causal link has not been established to date.

Electrogenic

A membrane transport process that involves net charge transfer accompanying substrate transport.

Electroneutral

A membrane transport process that involves no net charge transfer accompanying substrate transport.

Capacitive currents

Transient currents induced by changes in membrane potential that result from charging and discharging the membrane capacitance or displacement of mobile charges within the transmembrane electric field.

Voltage clamp fluorometry

(VCF). A technique in which time-resolved changes in fluorescence that reflect changes in the microenvironment of fluorophores linked to engineered cysteine residues at the periphery of the protein are measured. The changes in fluorescence can be interpreted as conformational changes induced by the membrane potential and cation availability.

Secondary topology

The orientation of membrane-spanning segments (for example, α-helices) and other secondary structures (for example, linkers and β-sheets) with respect to the inner and outer faces of the membrane.

Substituted cysteine accessibility (SCAM) technique

A technique used to determine secondary topological features by assessing the effect of linking methanethiosulfonate reagents to novel cysteines substituted at sites predicted to be of functional importance.

Repeat swap strategy

A homology modelling strategy applied to membrane transporters that contain repeat units. These are used as templates to predict alternative conformations not available from the crystal structure of the homologous protein.

K_i

The inhibitory constant for competitive inhibitors, which is related to the affinity of the inhibitor for the substrate binding site and is independent of the substrate concentration.

Na^+ slippage

An older term used to describe uncoupled Na^+ leak current mediated by Na^+-coupled transporters in the absence of substrate (for example, inorganic phosphate).

IC_{50}

The half-maximal inhibitory concentration — that is, the concentration of inhibitor that reduces transport (or other quantifiable physiological process) to a half at a specific concentration of the substrate that is being transported.

Figure 1

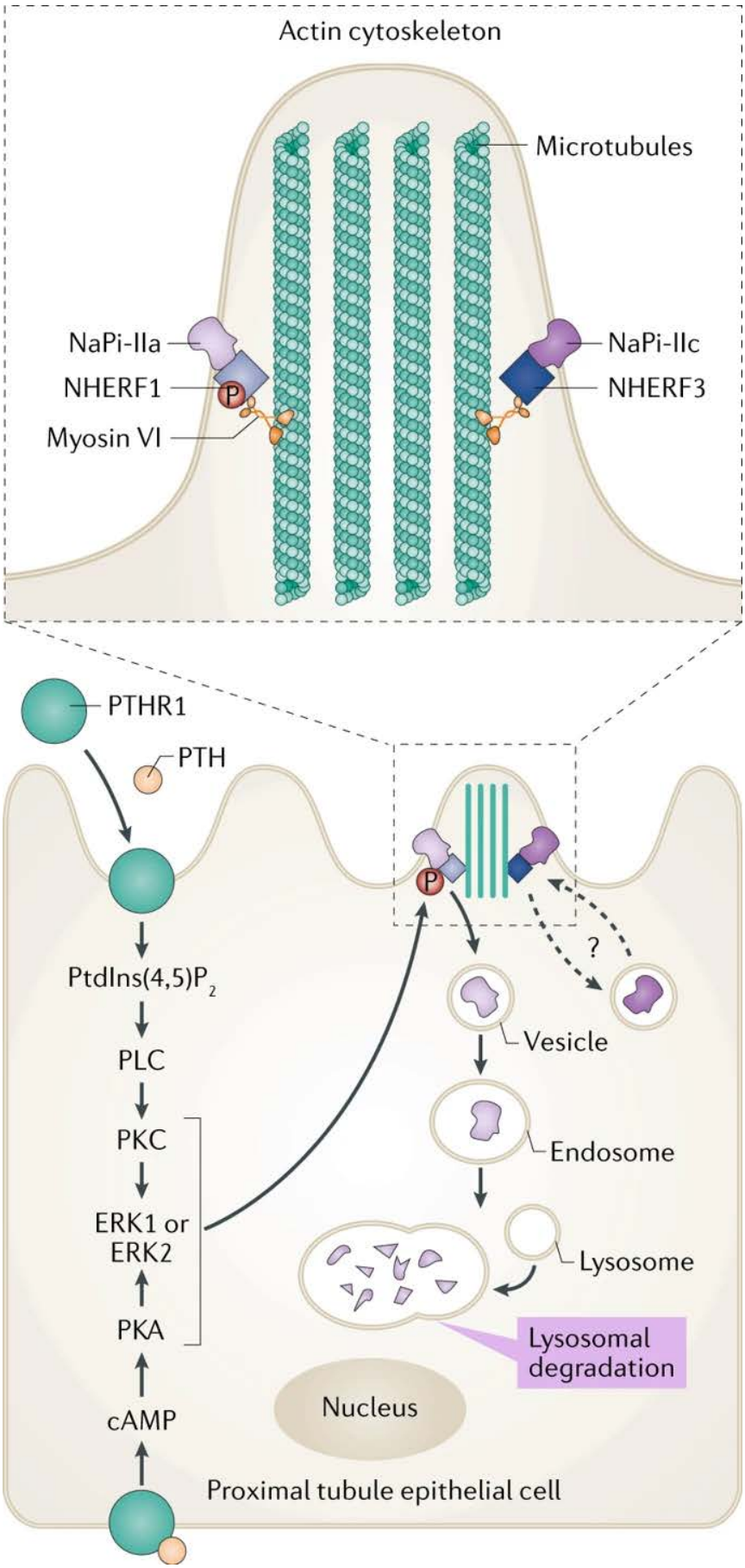
Actin cytoskeleton
Microtubules
NaPi-IIa
NHERF1
Myosin VI
NaPi-IIc
NHERF3
PTHR1
PTH
PtdIns(4,5)P2
PLC
PKC
ERK1 or ERK2
PKA
cAMP
?
Vesicle
Endosome
Lysosome
Lysosomal degradation
Nucleus
Proximal tubule epithelial cell

Figure 2

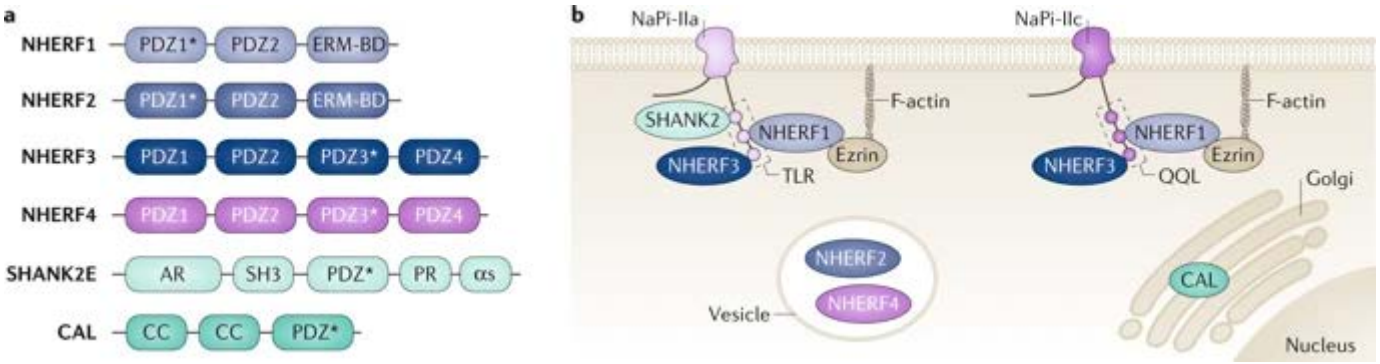
a
NHERF1
PDZ1*
PDZ2
ERM-BD
NHERF2
PDZ1*
PDZ2
ERM-BD
NHERF3
PDZ1
PDZ2
PDZ3*
PDZ4
NHERF4
PDZ1
PDZ2
PDZ3*
PDZ4
SHANK2E
AR
SH3
PDZ*
PR
αs
CAL
CC
CC
PDZ*
b
NaPi-IIa
NaPi-IIc
SHANK2
NHERF1
NHERF3
Ezrin
F-actin
TLR
QQL
Golgi
NHERF2
NHERF4
Vesicle
CAL
Nucleus

Figure 3

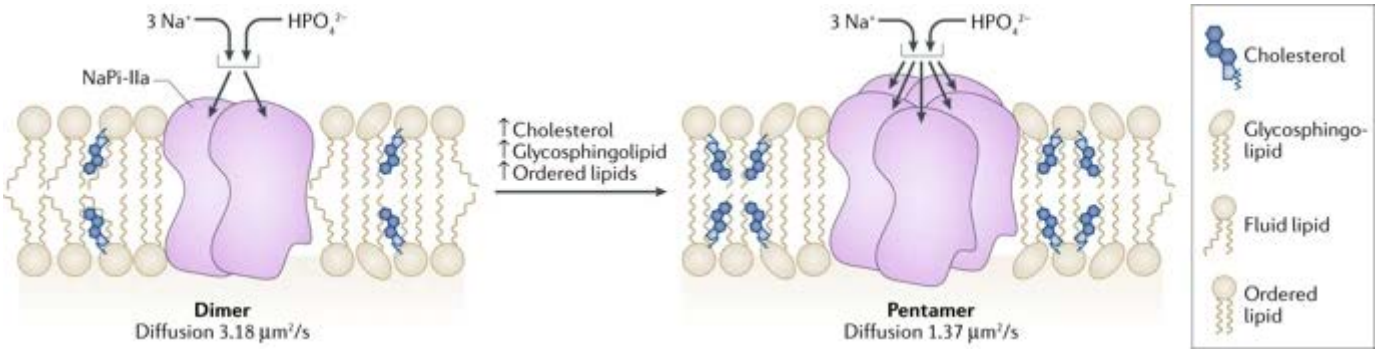
3 Na+
HPO4 2-
NaPi-IIa
Dimer
Diffusion 3.18 µm²/s
↑Cholesterol
↑Glycosphingolipid
↑Ordered lipids
3 Na+
HPO4 2-
Pentamer
Diffusion 1.37 µm²/s
Cholesterol
Glycosphingo-lipid
Fluid lipid
Ordered lipid

Figure 4

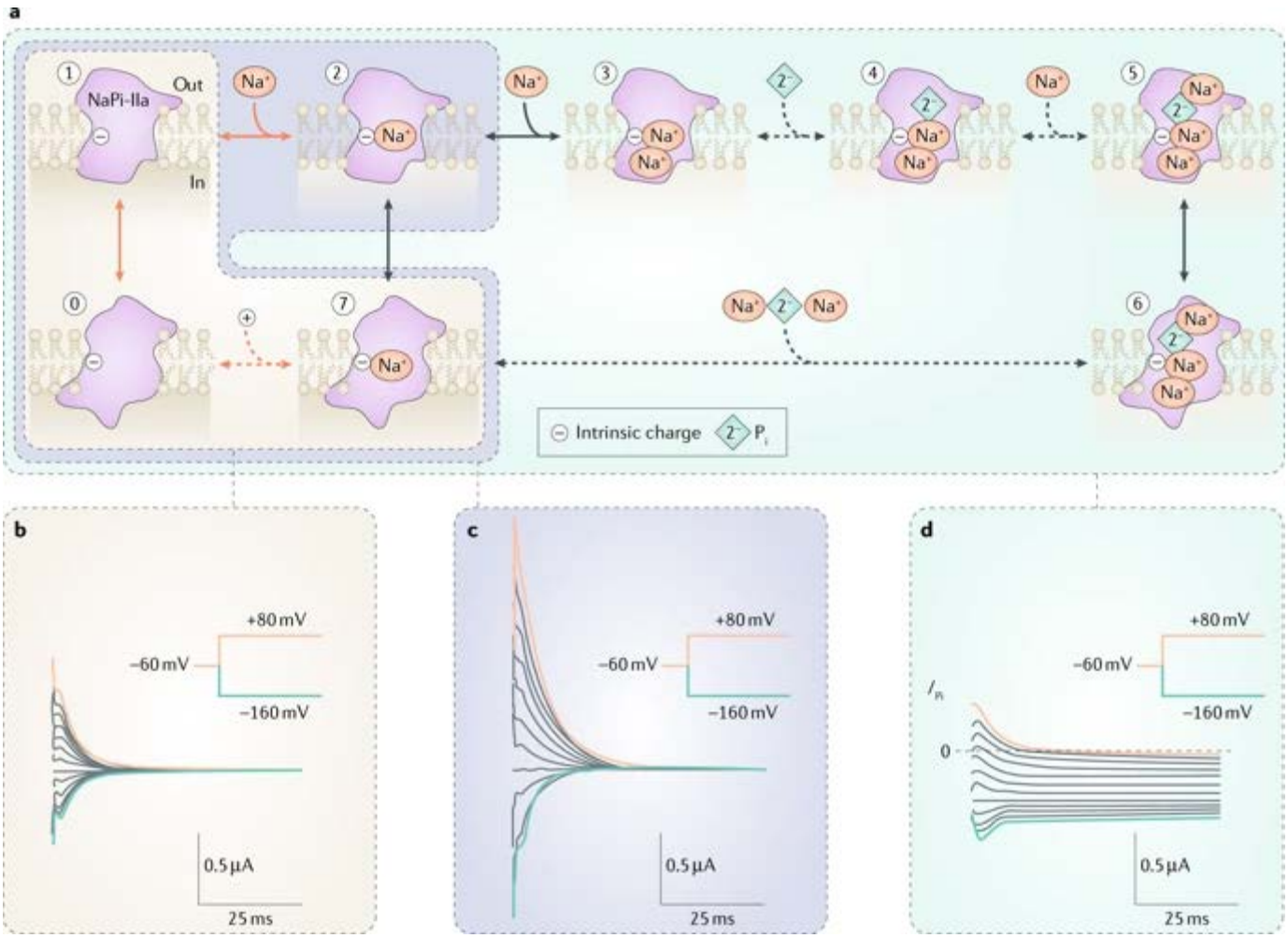
a
1
NaPi-IIa
Out
In
Na+
2
3
4
5
6
7
0
2-
Intrinsic charge
Pi
b
+80 mV
−60 mV
−160 mV
0.5 µA
25 ms
c
+80 mV
−60 mV
−160 mV
0.5 µA
25 ms
d
+80 mV
−60 mV
−160 mV
0
0.5 µA
25 ms

Figure 5

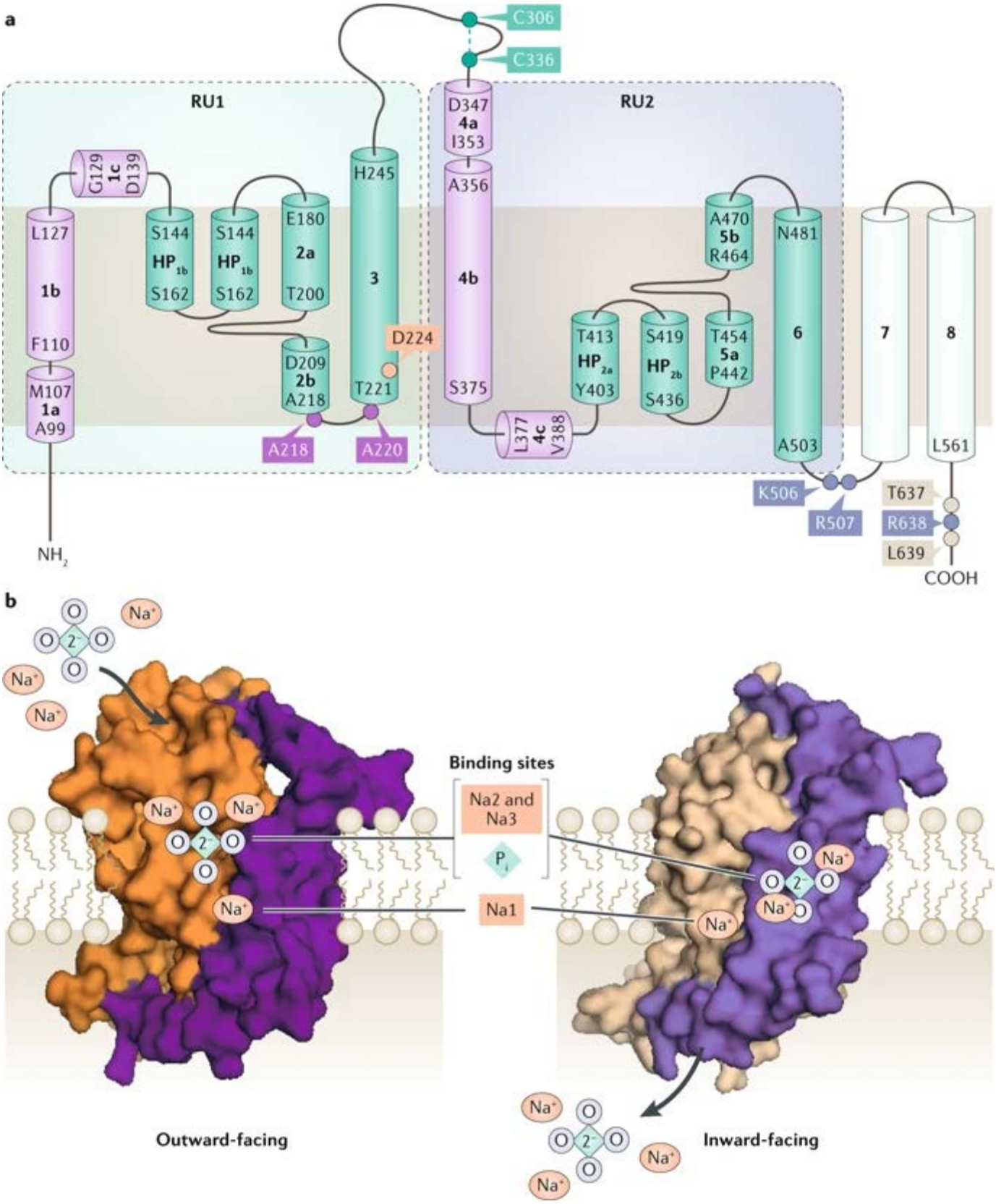
a
RU1
RU2
C306
C336
D347
4a
I353
A356
4b
S375
H245
3
T221
D224
G129
1c
D139
L127
1b
F110
M107
1a
A99
NH2
S144
HP1b
S162
S144
HP1b
S162
E180
2a
T200
D209
2b
A218
A218
A220
L377
4c
V388
T413
HP2a
Y403
S419
HP2b
S436
T454
5a
P442
A470
5b
R464
N481
6
A503
7
8
L561
K506
R507
T637
R638
L639
COOH
b
Na+
Binding sites
Na2 and Na3
Pi
Na1
Outward-facing
Inward-facing

Figure 6

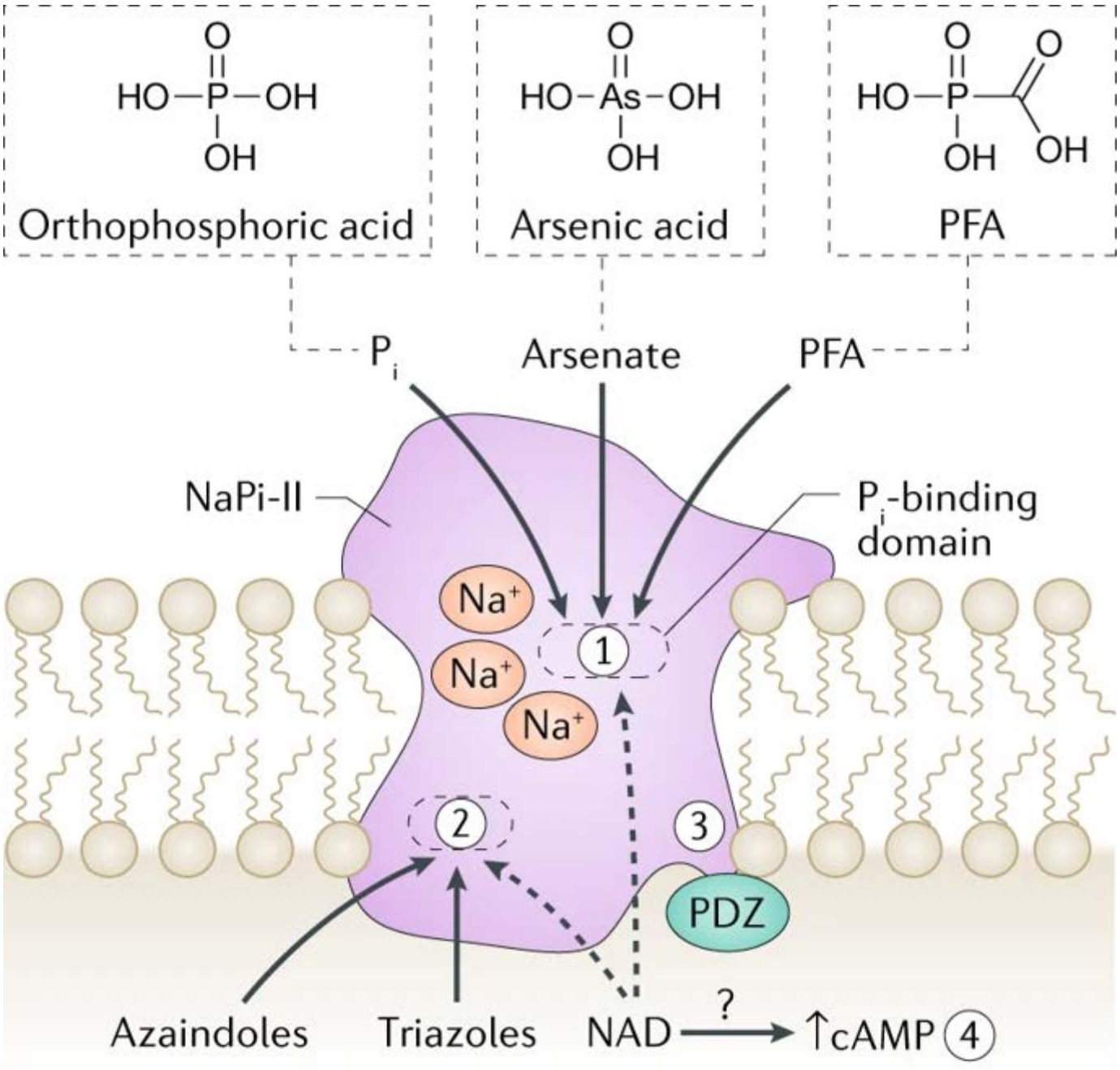
Orthophosphoric acid
Arsenic acid
PFA
P_i
Arsenate
PFA
NaPi-II
P_i-binding domain
Na^+
Na^+
Na^+
1
2
3
PDZ
Azaindoles
Triazoles
NAD
?
↑cAMP
4